博士論文

論文題目　**Effects of the ω-3 Polyunsaturated Fatty Acid, EPA, in Suppressing Abdominal Aortic Aneurysm Formation**

（腹部大動脈瘤の形成におけるω3多価不飽和脂肪酸[EPA]の抑制効果）

氏　　名　Jack Hung-Wen Wang（ジャック　ホン　ウェン　ワン）

Effects of the ω-3 Polyunsaturated Fatty Acid, EPA, in Suppressing Abdominal Aortic Aneurysm Formation

Department of Cardiovascular Medicine, Graduate School of Medicine
The University of Tokyo

Research supervisor: Professor Issei Komuro

Jack Hung-Wen Wang

CONTENTS

1. Abbreviations pp. 2

2. Abstract pp. 3 - 4

3. Introduction pp. 5 - 19

4. Materials and Methods pp. 20 - 31

5. Results

    5.1. Effects of EPA on aneurysmal tissue remodeling pp. 32 - 56

    5.2. Effects of EPA on vascular calcification in the aneurysm pp. 57 - 65

6. Discussion pp. 66 - 77

7. Acknowledgments p. 78

8. References pp. 79 - 93

1. ABBREVIATIONS

AAA	Abdominal aortic aneurysm
CCL	CC-chemokine ligand
COX	Cyclooxygenase
CT	Computed tomography
ECM	Extracellular matrix
EPA	Eicosapentaenoic acid
EVAR	Endovascular aneurysm repair
FACS	Fluorescence-activated cell sorting
FBS	Fetal bovine serum
IL	Interleukin
IP	Intraperitoneal
LPS	Lipopolysaccharide
MMP	Matrix metalloproteinase
NFκB	Nuclear factor κB
OPG	Osteoprotegrin
PBS	Phosphate buffered solution
PCR	Polymerase chain reaction
PG	Prostaglandin
PUFA	Polyunsaturated fatty acid
RANKL	Receptor activator of nuclear factor κB ligand
TIMP	Tissue inhibitors of metalloproteinase
TNF	Tumor necrosis factor

2. ABSTRACT

Abdominal aortic aneurysm (AAA) is a prevalent vascular disease that can rupture with a high rate of mortality. Inflammation and active remodeling of the aortic wall have been suggested to be critical in its pathogenesis. Omega-3 polyunsaturated fatty acids such as eicosapentaenoic acid (EPA) are known to reduce cardiovascular events, but its role in AAA management remains unclear. Here, I show that EPA attenuates murine $CaCl_2$-induced AAA development. AAA tissues from mice fed an EPA-diet appeared less inflamed and less calcified, and had relative preservation of aortic elastic lamina compared to those from mice in the Control diet group. AAA diameters were also significantly smaller in the mice fed an EPA-supplemented diet. Mechanistically, *Mmp9* mRNA levels and activity in the AAAs were reduced after EPA treatment. Consistent with this finding, RAW264.7 macrophages treated with EPA showed attenuated *Mmp9* levels after TNF-α simulation. Another effect exhibited by EPA was the suppression of AAA calcification, which was consistent with the reduction in levels of the vascular calcification factor *Rankl* (*Tnfsf11*) in the mice treated with EPA. Up-regulation of *Rankl* and *Mmp9* levels was found to be temporally related in the early phases of AAA formation, and recombinant RANKL protein was shown to induce

Mmp9 expression in cultured peritoneal macrophages. These results demonstrate a novel role of EPA in attenuating AAA formation via the suppression of macrophage-derived MMP-9 as well as possibly via the suppression of aneurysmal *Rankl* expression levels, and raise the possibility of using EPA for AAA prevention in the clinical setting.

3. INTRODUCTION

Abdominal aortic aneurysm (AAA) is a disease involving the gradual and irreversible dilatation of the abdominal aorta [1]. While aneurysms can technically affect any part of the abdominal aorta, the term AAA is generally reserved for aneurysms of the infra-renal aorta, which is by far the most common site of aneurysm formation. Abdominal aortic aneurysms are common particularly in men older than 65 years of age and has a reported prevalence of 4-9% in men and 1% in women [2,3]. The most important risk factors for developing the disease are advanced age, smoking, and male gender [3,4]. Natural disease progression of untreated AAAs result in a high risk of aneurysm rupture that has an associated mortality rate as high as 65% to 85% [3]. Therefore, current consensus on the clinical management of AAAs focuses on the early diagnosis, monitoring, and if required, treatment of AAAs prior to rupture. However, while AAAs can be easily detected with an imaging modality such as abdominal ultrasound, diagnosis of this disease in its early stages prior to rupture remains difficult because most patients do not present for clinical assessment as AAAs often remain asymptomatic or are only associated with non-specific symptoms such as lower back pain. Patients are commonly diagnosed with AAAs incidentally during routine medical

checkups or as part of AAA screening programs, particularly in those identified as being at high risk of the disease.

The most commonly accepted clinical definition of an AAA is when the maximum infra-renal abdominal aortic diameter exceeds 3.0 cm, although definitions that use a maximum abdominal aortic diameter of more than 1.5 times that of the expected normal diameter has also been proposed [4]. While current guidelines in the clinical management of AAA remain region-specific across the world and each differs in certain aspects, the major consensus that these guidelines share is to tailor management based on the size of AAAs. In particular, most guidelines stipulate that patients with a maximum infra-renal aortic diameter of 5.5 cm or greater should be referred to a vascular surgeon for consideration of treatment, as evidence has firmly established that AAAs larger than this have an exponential increase in the annual rate of rupture of 10% to 22% that is much greater than the typical rates of complication of elective AAA repairs [4,5]. Treatment options remain limited, however, with open surgical repair or minimally invasive endovascular aneurysm repair (EVAR) being the only definitive and curative treatment options for AAAs to date. Open surgical repair, as the name suggests, involves a laparotomy, excising the aneurysmal tissue, and replacing with an aortic graft. In contrast, EVAR was developed as a minimally invasive procedure that involves

inserting a stent-graft via the femoral arteries into the aneurysmal lumen first, followed by deployment of the stent-graft within the AAA so that the graft excludes the aneurysmal sac from the circulation. This leads to a reduction in pressure on the aneurysmal sac, which over time eventually undergoes thrombosis and decreases in size [6]. The choice of treatment is typically dependent on several factors, such as clinical characteristics of the patient (for example, whether or not the patient could cope with a prolonged surgical repair, presence of comorbidities that would preclude the patient from surgery, etc.), the anatomical characteristics of the AAA itself, and patient preference. However, as AAAs are mostly a disease of the elderly, patients often have numerous comorbidities (for example, concomitant cardiovascular or renal disease) that reduce their suitability for surgical repair, leaving them with even fewer treatment options in reality.

In light of the current limitations in surgical treatment, emphasis of current basic and clinical research has focused on trying to uncover pharmacological therapies that may be useful in the prevention or slowing of AAA development, thereby delaying or circumventing completely the need for surgical intervention. A number of pharmacological agents have been shown to suppress AAA formation in experimental animal models including statins, angiotensin-converting enzyme (ACE) inhibitors,

antibiotics, beta blockers, and anti-inflammatory agents. Given their potential in limiting AAA progression, many of these agents have been investigated in various human clinical trials [4,7,8]. However, results of most of the completed trials have been disappointing in that the studied medical treatments had either no or only marginal benefits in retarding aneurysm expansion [7,9-12]. While the administration of some of these agents are nevertheless recommended in the optimal medical management of patients with diagnosed AAAs, there remains an urgent need for a new and more effective pharmacological therapy to be discovered for the prevention or slowing of AAA development.

Over the last two decades, our understanding of the pathological mechanisms underlying AAA development has improved dramatically. This is in part due to the advent of animal models of AAA that has allowed researchers to investigate the mechanisms of aneurysmal formation ever more closely and without having to use human tissues, which is often a rare resource. There are currently three major animal models of AAAs commonly used in this research field. The first is the induction of murine AAA formation by the direct perivascular application of calcium chloride ($CaCl_2$) to the infra-renal aorta in mice. This was a modification of a technique originally reported by Gertz *et al* 25 years ago that was used to induce aneurysm

formation in rabbit common carotid arteries, which has since been adapted for use in murine abdominal aortas [13,14]. By eliciting an inflammatory reaction in abdominal aortas with $CaCl_2$, the authors were able to obtain a doubling in the diameter of the infra-renal abdominal aorta over a 3 week period after the AAA surgery. The second animal model involves the continuous infusion of angiotensin II via subcutaneous osmotic pumps into $ApoE^{-/-}$ or LDL $receptor^{-/-}$ mice over a 3 to 4 week period [15]. By virtue of their genetic deficiencies of ApoE or LDL receptor, these mice have deranged lipid profiles and were surprisingly found to produce AAAs with a high incidence upon additional angiotensin II infusion. However, these AAAs are typically located in the supra-renal abdominal aorta, a position that is markedly different from the most common infra-renal site of human AAA disease. The third model is also a chemically-induced AAA model that involves the direct infusion of elastase into the infra-renal aorta. Elastase is infused via a micro-catheter inserted into the infra-renal aorta at the level of the iliac bifurcation while the infra-renal aorta is temporarily ligated at a level just below the renal arteries [16]. Elastase infused into the aorta disrupts and destroys aortic elastic fibers, thereby leading to structural vascular wall weakness, inflammation, and gradual AAA formation [16,17]. While each of these models differ in methodology and their individual mechanistic pathways may not all be the same, some

central features, such as medial aortic wall degeneration and inflammatory response, are shared across all three models. Despite some differences, these models have nevertheless been utilized widely, with many of their findings translated to and confirmed in human diseases as well.

Pathohistologically, the hallmark features of AAAs are the fragmentation of elastin, which forms the elastic fibers that give arteries their elastic properties, and loss of collagen, which provides tensile strength and maintain arterial structural integrity [3]. Loss of these connective tissue components within the abdominal aortic wall lead to reduced vascular wall strength and eventual arterial dilatation, resulting in the formation of an AAA. These fibers can be degraded by proteases, the most notable of which are the matrix metalloproteinases (MMPs). MMPs are a family of zinc-dependent endopeptidases that under normal conditions possess a variety of physiological functions ranging from tissue remodeling to organ development [18]. MMPs are secreted first in an enzymatically inactive “proform” state that becomes proteolytically active once it is cleaved by other MMPs or serine proteinases [18,19]. In addition, and more importantly, the proteolytic activities of MMPs in tissues are also regulated by their physiological inhibitors, tissue inhibitors of metalloproteinases (TIMPs) [18]. The

balance between tissue levels of MMPs and TIMPs thus maintains the degree of proteolysis within physiologically acceptable ranges.

The first reports that described the presence of MMPs such as MMP-1, MMP-2, MMP-3, and MMP-9 in human AAA samples emerged in the 1990s, when it became clear that these enzymes were clearly associated with AAA development [20-23]. At around the same time, it was also demonstrated that a variety of immune cells accumulate in AAAs [24]. Together, these results began to paint a picture where AAA formation in fact involves the orchestrated interactions between inflammatory immune cells and proteolytic factors, thereby resulting in aortic connective tissue destruction and eventual rupture. Numerous studies since then have revealed that inflammatory cells and processes play a key role in the development of AAAs. Beginning with the demonstration by Newman *et al* that MMP-9 co-localized to macrophages, the professional phagocytic cells of the innate immune system, within human AAA samples [22], Pyo *et al* and Longo *et al* went on to show that development of AAAs is ameliorated in mice genetically deficient in MMP-2 or MMP-9 in their respective landmark reports [16,25]. This and other subsequent studies provided the first and direct causal evidence of the critical role of macrophage-derived MMP-9 and vascular smooth muscle cell (VSMC)-derived MMP-2 in the pathogenesis of AAA [3,25,26].

Macrophages are major phagocytic cells that play critical and central roles in the innate immune system. Their importance in many aspects of disease biology, ranging from tumor angiogenesis [27] through to obesity and metabolic syndrome [28], has been revealed over the last two decades. As a result, our understanding of these cells and their numerous subtypes has also increased in an exponential fashion. The developmental cascade of macrophages has been well defined. Tissue-resident macrophages that contribute to the maintenance of tissue homeostasis are known to be derived from circulating monocytes [29,30]. These monocytes originate from defined myeloid progenitor cells in the bone marrow, and after undergoing a series of lineage-committed steps of cellular differentiation, are subsequently released into the circulation as monocytes. From there, these monocytes enter peripheral tissues to maintain constant numbers of tissue-resident macrophages. Monocytes express the myeloid cell surface markers CD11b and Ly-6C [29]. In particular, monocytes are known to express Ly-6C in high levels (Ly-6C^{hi}), but upon entering tissues to become tissue-resident macrophages their Ly-6C expression markedly decreases to a low level (Ly-6C^{low}) [29]. In addition, they also begin to express the macrophage marker F4/80 during the process of monocyte-macrophage differentiation in tissue, thereby making these cell surface markers useful for distinguishing monocytes from macrophages.

Besides replenishing tissue-resident macrophages during homeostasis, monocytes can also be actively recruited during the tissue inflammatory response. In response to chemoattractant cytokines such as CC-chemokine ligand 2 (CCL2) produced by the inflamed tissue, Ly-6C^{hi} monocytes in the circulation are actively recruited to and enter the tissue to clear pathogens and necrotic tissue as well as orchestrate wound healing by becoming macrophages. In recent years it has become evident that these inflammatory responses are not mediated by a single, homogeneous pool of macrophages, but rather by distinct macrophage subtypes that perform particular roles in a specific, temporally and spatially regulated manner. There are two, broad subtypes: classically activated, inflammatory "M1" macrophages and alternatively activated, wound-healing "M2" macrophages. This classification is by no means exhaustive, and numerous studies have shown that other minor macrophage subtypes with distinctively different functions exist as well [31]. Nevertheless, the M1/M2 paradigm is a useful platform for understanding macrophage function in tissue inflammation and its resolution. Monocytes recruited in the initial stages of inflammation become inflammatory M1 macrophages which, as their name suggests, produce major pro-inflammatory cytokines such as tumor necrosis factor (TNF)-α, interleukin 6 (IL6), and CCL2, and possess enhanced microbicidal as well as phagocytic

activities so that they may carry out their role in host defences and mediate the events that occur during the acute phase of tissue inflammation [31]. As this acute phase subsides, the proportion of wound-healing M2 macrophages increases relative to M1 macrophages [32]. These M2 macrophages are characterized by the up-regulation of markers such as arginase 1 (ARG1) and mannose receptor C type 1 (MRC1, also known commonly as CD206), and they play an important role in the orchestration of the resolution of tissue inflammation as well as tissue fibrosis that occurs due to an effort by the body to heal the wound left over after the inflammatory reaction.

Besides macrophages, various other reports have also provided evidence of the involvement of many other immune cells in the development of AAAs by using the aforementioned animal models of the disease. These immune cells include T cells [33,34], neutrophils [35], and mast cells [36]. In particular, Shimizu *et al* [37] demonstrated that a specific subset of $CD4^+$ T cells, otherwise known as T helper (T_h) cells, are particularly important for AAA formation. T_h cells can differentiate into two major subtypes of effector cells known as T_h1 or T_h2 cells. T_h1 cells produce T_h1 cytokines such as interferon (IFN)-γ that promote cellular inflammatory responses, whereas T_h2 cells produce T_h2 cytokines such as IL4 that are important for driving specific immunological processes including allergic responses and asthma [34]. The

results of the report from Shimizu *et al* [37] suggest that a T_h2 environment may promote the formation of AAAs. This is an interesting factor to consider from the experimental point of view, given that different strains of mice have been reported to harbor different T_h phenotypes. For example, the most commonly used mouse strain C57BL/6 is known to be skewed towards a predominantly T_h1 phenotype, whereas BALB/c mice are reported to be skewed towards a T_h2 phenotype. Indeed, AAAs spontaneously formed when Shimizu *et al* [37] transplanted aortic segments from T_h1 polarized mice into BALB/c mice, thereby demonstrating the importance of T_h2 signaling pathways in the pathogenesis of AAAs. This suggests that the choice of mouse strain when performing studies in experimental murine AAAs can also be a major factor in affecting the outcome of the study.

Calcification is commonly found in various diseases such as chronic kidney disease, atherosclerosis, and diabetes mellitus [38]. Indeed, AAAs are also often observed to be associated with calcification [1], although the significance of calcification in relation to AAA formation has not been reported. Our understanding of the mechanisms underlying vascular calcification in general has markedly improved over recent years. It is now well established that certain members of the TNF family of cytokines are intimately associated with the pathogenesis of vascular calcification.

Receptor activator of nuclear factor kappa-B ligand (RANKL), otherwise also known as TNFSF11, encodes a protein that is involved in the maintenance of bone homeostasis and metabolism. RANKL functions in the differentiation and activation of osteoclasts (bone-resorbing cells), as well as T cell and B cell maturation, and is typically only expressed weakly throughout the vascular system under physiological conditions [39]. However, its expression can be greatly up-regulated in calcified or atherosclerotic vascular lesions especially when in the presence of calcium or cytokines such as IL6 or IL17 [39]. RANKL binds to its receptor, the receptor activator of nuclear factor kappa-B (RANK), which is normally found on monocyte/macrophage lineage cells; however, RANK expression can also be up-regulated in endothelial cells and vascular smooth muscle cells (VSMC) in a similar manner to RANKL [39]. In the setting of vascular calcification, RANKL has been reported to activate RANK on VSMCs to lead to the nuclear translocation of nuclear factor κB (NFκB), the well-known master regulator of cellular responses to infection and inflammation, via an alternative activation pathway involving BMP4 and cause calcification to occur [38]. Meanwhile, osteoprotegin (OPG) is an endogenous decoy receptor that inhibits all functions of RANKL. Unlike RANKL and RANK, OPG is constitutively expressed throughout the cardiovascular system. The importance of the balance between levels of RANKL and OPG in vascular calcification

is exemplified by studies that showed the development of severe vascular calcification in mice with a genetic deficiency in OPG, where RANKL levels increased with unopposed function in the vascular system. In addition to the RANKL-OPG axis, recent studies have also revealed that Runx2, a master osteogenic transcription factor, up-regulates the expression of RANKL in VSMC by directly binding to its promoter region and thereby lead to vascular calcification [40]. Indeed, this is further supported by *in vivo* studies that showed that mice with a smooth muscle cell (SMC)-specific genetic deficiency in Runx2 had markedly suppressed vascular calcification associated with atherosclerosis [41]. These studies provide strong evidence for the involvement of RANKL, OPG, and Runx2 in vascular calcification, although their involvement in AAAs has not been reported yet.

Omega-3 (ω-3) polyunsaturated fatty acids (PUFAs) are a class of essential fatty acids required for normal biological activity and function in living organisms. These fatty acids are named “polyunsaturated” due to the presence of two or more double bonds in their carbon chain chemical structure. Moreover, the designation “ω-3” denotes the fact that the first double bond is found at the third carbon atom from the omega end of the carbon chain, distinguishing these fatty acids from ω-6 and ω-9 PUFAs. These fatty acids can typically be either plant-derived (α-linolenic acid) or

marine fish-derived [eicosapentaenoic acid (EPA) and docosahexaenoic acid (DHA)] [42]. From numerous clinical, epidemiological, and animal studies, ω-3 PUFAs have been demonstrated to possess anti-inflammatory [43,44], anti-fibrotic [45], and cardioprotective properties [46,47], and they are already being used widely as pharmacological agents and nutritional supplements in humans. They have been suggested to have various mechanisms of action, including the ability to reduce the production of inflammatory eicosanoids by competing with arachidonic acid [42], exertion of anti-inflammatory effects via ligand-receptor interactions with the G protein-coupled receptor 120 [44], and activation of the active resolution of inflammation by ω-3 PUFA metabolites such as resolvin E1 and protectin D1 [48]. However, despite advances in our understanding of effects of ω-3 PUFAs, the precise molecular mechanisms as to how they exhibit beneficial effects in each pathological process still remain to be elucidated.

The role of ω-3 PUFAs in the management of AAAs has not been established. Given the pleotropic properties of ω-3 PUFAs, I hypothesized that ω-3 PUFA might also suppress the formation of AAAs by attenuating tissue remodeling processes. By using $CaCl_2$ to induce the development of AAAs in mice, I show that EPA can attenuate the formation of AAAs in the $CaCl_2$-induced AAA model by suppressing tissue remodeling

processes. In addition, I also show that EPA suppressed vascular calcification in the AAA by attenuating the up-regulation of *Rankl* elicited by $CaCl_2$.

4. MATERIALS AND METHODS

Mice

Male 7 to 9 week-old BALB/cA mice were purchased from CLEA Japan (Tokyo) and kept in a temperature and humidity controlled room with a 12-hour light and 12-hour dark cycle. Mice were allowed unrestricted access to either a Control diet (fish meal-free F1 chow, 362 kcal/100 g with 4.4% energy as fat; Funabashi Farm, Chiba) or an EPA-supplemented diet (Control diet supplemented with 10% wt/wt EPA), and preparation of the diets has been described elsewhere [49]. Briefly, ultrapure EPA (>98.0% EPA) capsules were opened and the liquid EPA emptied into the fish meal-free F1 chow in a Ziploc® freezer bag. The amount of EPA and F1 chow added was calculated to produce an EPA-supplemented diet with a final concentration of 10% wt/wt of EPA. The freezer bag was closed and the contents inside well mixed by hand for five to ten minutes. The contents were then served in glass feeders to reduce the rate of oxidation of EPA. Control diet was also served in the same type of glass feeder. All experimental diets were freshly made once every two to three days. Ultrapure EPA was generously provided by Mochida Pharmaceuticals Co., Ltd. (Tokyo).

The $CaCl_2$-induced AAA model was performed as previously described [19,25]. Briefly, 4 days after the experimental diets were commenced, periaortic application of 500 mmol/L $CaCl_2$ (Sigma-Aldrich) for 15 minutes was performed in mice anaesthetized with intraperitoneal (IP) pentobarbital injection to induce AAA formation. For mice that received sham surgery, NaCl instead of $CaCl_2$ was applied periaortically for the same period of time. Mice continued their experimental diets until sacrifice for analysis. At the 6-week time point, infra-renal aortas were photographed under microscopy prior to harvesting and the external aortic diameter was determined by a blinded observer according to a previously described method [14]. All experiments were approved by the University of Tokyo Ethics Committee for Animal Experiments and strictly adhered to the guidelines for animal experiments of the University of Tokyo.

Histological analysis

Mice were first anaesthetized with IP pentobarbital injection and then perfused with 10 mL ice cold PBS per mouse via cardiac puncture. Following this, mice were perfusion-fixed with 20% Tissue-Tek UFIX (Sakura Finetek Japan), again via cardiac puncture. The infra-renal aortas were then harvested, further fixed in 20% Tissue-Tek

UFIX, dehydrated, embedded in paraffin, and sectioned. Histological analysis was performed by Elastica van Gieson staining according to standard procedures.

In vivo micro-CT imaging

Six weeks after induction of AAA formation by $CaCl_2$, mice were anaesthetized with IP pentobarbital injections and IV contrast (ExiTron nano 6000, Miltenyi Biotec) was administered via the tail vein. While anaesthetized, the mice were subjected to micro-CT imaging with the LaTheta LCT-200 CT scanner (Hitachi Aloka Medical, Ltd.). After the procedure, mice were sacrificed to harvest infra-renal aortas for further analysis. Quantification of aortic calcification was performed by taking 30 slices of the same anatomical section of infra-renal aorta in each animal and calculating the volume of calcification using the scanner's standard image analysis software.

Quantitative real-time PCR analysis

Mice were first anaesthetized with IP pentobarbital injection and then perfused with 10 mL ice cold PBS per mouse via cardiac puncture. Infra-renal aortas from control- or EPA-diet-fed mice were harvested and placed immediately into RNAlater (Ambion) to preserve tissue RNA integrity. Total RNA was purified from aortic tissues

using the RNeasy Fibrous Tissue Mini kit (Qiagen), and using the RNeasy Plus Micro Kit (Qiagen) for cells sorted by flow cytometry, according to the manufacturer's instructions. For the purification of RNA from cultured cells, RLT buffer with β-ME (Qiagen) was added to the cells directly, harvested, and subjected to homogenization with the QIAShredder (Qiagen). Subsequent RNA purification was performed using the RNeasy Mini kit (Qiagen) according to the manufacturer's instructions. RNA concentrations were measured using the NanoDrop 1000 spectrophotometer (Thermo Scientific). Complementary DNA was synthesized using 200 ng to 1000 ng of RNA in 10 μl per sample with the SuperScript III First-Strand Synthesis System (Invitrogen). Quantitative real-time PCR analyses were conducted using the QuantiTECT SYBR Green PCR kit (Qiagen) with the LightCycler system (Roche). *18s* rRNA served as the internal control in all experiments. Primer sequences of the analyzed genes are listed in Table 1, and were designed using the Roche Universal Probe Library Assay Design Center (based on Primer3).

Table 1. Primer sequences of the genes analyzed by quantitative real-time PCR.

Gene	***Forward primer (5' to 3')***	***Reverse primer (5' to 3')***
Ccl2	CAT CCA CGT GTT GGC TCA	GAT CAT CTT GCT GGT GAA TGA GT
Col1a1	CAT GTT CAG CTT TGT GGA CCT	GCA GCT GAC TTC AGG GAT GT
Col3a1	TCC CCT GGA ATC TGT GAA TC	TGA GTC GAA TTG GGG AGA AT
Fn1	CGG AGA GAG TGC CCC TAC TA	CGA TAT TGG TGA ATC GCA GA
Mmp2	TAA CCT GGA TGC CGT CGT	TTC AGG TAA TAA GCA CCC TTG AA
Mmp9	ACG ACA TAG ACG GCA TCC A	GCT GTG GTT CAG TTG TGG TG
Opg	GTT TCC CGA GGA CCA CAA T	CCA TTC AAT GAT GTC CAG GAG
Rankl	TGA AGA CAC ACT ACC TGA CTC CTG	CCA CAA TGT GTT GCA GTT CC
Runx2	TCC ACA AGG ACA GAG TCA GAT TAC	TGG CTC AGA TAG GAG GGG TA
Timp1	GCA AAG AGC TTT CTC AAA GAC C	AGG GAT AGA TAA ACA GGG AAA CAC T
Timp2	CGT TTT GCA ATG CAG ACG TA	GGA ATC CAC CTC CTT CTC G

Zymography

Zymography is a simple technique that can be used to detect the functional activity of MMPs present in tissue or cellular samples. For the assessment of MMP activity in AAAs, mice were first anaesthetized with IP pentobarbital injection and then perfused with 10 mL ice cold PBS per mouse via cardiac puncture. Infra-renal aortas from mice in the Control diet or EPA diet groups were harvested and placed immediately into liquid nitrogen. The frozen samples were homogenized in 2X lysis buffer (containing 50 mmol/L Tris/HCl [pH7.5], 150 mmol/L NaCl, 1.0% IGEPAL CA-630, 2 mmol/L EDTA) combined in a 1:1 ratio with 25X cOmplete EDTA-free protease inhibitor cocktail (Roche Diagnostics). Protein concentration of each aortic extract was determined with the DC Protein Assay (Bio-Rad). Zymography was performed as previously described [50]. Briefly, 20 μg of total protein was equally loaded onto each well of a Novex 10% Zymogram (gelatin) gel (Invitrogen) and separated under non-reducing conditions at 125 V constant until the indicator dye reached the bottom of the gel. The gels were then removed from the cassette, renatured in renaturing buffer (2.5% vol/vol Triton®X-100 solution), developed with Novex Zymogram Developing Buffer (Invitrogen), and stained with SimplyBlue SafeStain (Life Technologies) for analysis. The gels were scanned using a standard digital scanner

at 300 dpi and the intensity of bands corresponding to MMPs were analyzed using Image J (U. S. National Institutes of Health) image analysis software.

Flow cytometric analysis and cell sorting

For flow cytometric analysis of AAAs, mice were first anaesthetized with IP pentobarbital injection and then perfused with 10 mL ice cold PBS per mouse via cardiac puncture. Infra-renal aortas from control- or EPA-diet-fed mice were harvested and placed immediately into PBS on ice. Three fresh, isolated infra-renal aortas from the same experimental group were pooled into one sample for flow cytometric analysis. Pooled samples were finely cut and placed in Hank's balanced salt solution (with Ca^{2+} and Mg^{2+}) containing 400 U/mL collagenase type II (Worthington Labs), 0.75 U/mL elastase (Worthington Labs), and 60 U/mL DNase I (Sigma-Aldrich) at 37°C for one hour with shaking to dissociate the aortic tissue into single cells. Cell pellets were washed twice with ice cold FACS buffer (PBS containing 5% fetal bovine serum [FBS]) and suspended in 100 μL FACS buffer per 1 x 10^5 cells followed by flow cytometric analysis according to standard procedures.

For flow cytometric analysis of peripheral blood, mice were first anaesthetized with IP pentobarbital injection and laparotomy was performed. Approximately 300 μL

of peripheral blood was obtained via the inferior vena cava using a 30-G insulin syringe that contained 10 μL of 1 U/mL heparin/PBS mixture (heparin from Ajinomoto Pharmaceuticals). The blood was then added to a 1.5 mL Eppendorf tube containing 1 mL of 1 U/mL heparin/PBS mixture and placed at room temperature while the procedure was repeated for all other samples. The samples were then centrifuged at 2000 rpm for 2 minutes at room temperature. The supernatant was discarded and 1 mL of 1.2% wt/vol dextran/PBS mixture (dextran sulphate sodium salt from Amersham) was added and the mixture placed at room temperature for 45 minutes. The supernatant was then transferred to a new 5 mL polystyrene Falcon round-bottom tube (BD Falcon) and centrifuged at 2000 rpm for 2 minutes at 4°C. The supernatant was discarded and 1 mL hemolytic buffer (to remove erythrocytes; composed of 100 mM NH_4Cl and 17 mM Tris-HCl, pH 8.0, in distilled H_2O) was added to the cell pellet and left on ice for 3 minutes. Approximately 3 mL FACS buffer was then added to the mixture and centrifuged at 2000 rpm for 5 minutes at 4°C. After discarding the supernatant, 3 mL of FACS buffer was again added to the cell pellet and centrifuged at 2000 rpm for 2 minutes at 4°C. The supernatant was discarded and the cell pellet suspended in approximately 300 μL FACS buffer followed by flow cytometric analysis according to standard procedures.

For both protocols, after suspension of the cell pellet in FACS buffer, 10 μL of the cell suspension was removed for cell counting using the Countess® Automated Cell Counter (Invitrogen) prior to performing Fc blocking. One microliter Fc block (BioLegend) per 100 μL of cell suspension was added and incubated on ice for at least 15 minutes. The primary antibodies were then added at 1 μL per 100 μL cell suspension and incubated on ice for 30 minutes. The cell suspension and antibody mixture was then washed twice with ice-cold FACS buffer and filtered into a 5 mL polystyrene Falcon round-bottom tube with cell-strainer cap (BD Falcon). The final cell pellet was suspended in 1 mL FACS buffer and analyzed using the FACSAria II (BD). The antibodies used for the analyses were anti-CD11b (clone M1/70) from eBioscience; anti-F4/80 (BM8), anti-Ly-6C (HK1.4), and anti-Ly-6G (1A8) from BioLegend, as well as the corresponding isotype controls for each antibody.

Giemsa staining of flow cytometry sorted cells

Cells sorted by flow cytometry were placed onto microscope slides by centrifuging the cells at 1000 rpm for 3 minutes in the Cytospin 4 (Thermo Scientific). The cells were then fixed with ice cold 100% methanol and air-dried. Giemsa staining was then performed with Giemsa's azur eosine methylene blue stain (Merck) that had been 10X

diluted in 1X pH6.4 PBS solution. Thirty minutes after staining, the cells were observed under the microscope.

Peritoneal macrophages

Peritoneal macrophages were obtained as previously reported [51] with some modifications. Male BALB/cA mice aged 8-10 weeks were IP injected with 2.5 mL of 3% thioglycollate medium (BD Difco). Four days later, the elicited peritoneal macrophages were harvested by first sacrificing the mice and thoroughly sterilizing their abdominal surface with 70% alcohol. A skin incision over the abdomen was made, being careful not to puncture the underlying peritoneal lining, and 6 mL of ice cold PBS was injected into the abdominal cavity and aspirated. This procedure was repeated twice to obtain approximately 10 mL of PBS containing peritoneal cells. After the cells were centrifuged at 1000 rpm at 4^{o}C, the supernatant was aspirated and the cell pellet was resuspended in culture medium. Cells were plated at 3×10^{5} cells / cm^{2} in 6-well plates so as to give a final cell confluency of 70 to 80%. Two to three hours after plating, the medium was changed and plated cells were ready to use for experimentation.

Cell culture

Murine RAW264.7 macrophages were obtained from American Type Culture Collection and cultured in Dulbecco's modified Eagle's medium (DMEM; Gibco) supplemented with 10% FBS (Hyclone). Thioglycollate-elicited peritoneal macrophages were cultured in DMEM/F12 medium supplemented with 10% FBS (Hyclone). All cells were cultured at 37^{O}C with 5% CO_2.

For the *in vitro* treatment of RAW264.7 macrophages with EPA, RAW264.7 macrophages were plated at 4 x 10^4 cells / cm^2 in 12-well plates and used immediately after plating. Stock solutions of 150 mmol/L EPA (Cayman Chemical) were prepared and stored according to the manufacturer's instructions until use. Culture medium containing EPA was prepared according to previously described methods for fatty acid preparation, with some minor modifications [52]. Briefly, aliquots of the stock solution of EPA were complexed with fatty-acid-free, low-endotoxin bovine serum albumin (BSA; 10% wt/vol solution in H_2O, Sigma-Aldrich) to give a 7.5 mmol/L working solution, which was incubated at 37°C for 30 minutes. After incubation, the working solution was added to warmed DMEM (supplemented with 10% FBS) to give a final concentration of 10, 25, or 50 μmol/L. The vehicle solution was prepared similarly using a mixture of ethanol/water instead of EPA, and this was used as the vehicle

control. After 48 hours of treatment with vehicle- or EPA-containing medium, 20 ng/mL of recombinant mouse TNF-α protein (R&D Systems) was added and cells were harvested for analysis.

For stimulation of peritoneal macrophages with mouse recombinant RANKL protein (Miltenyi Biotec), the required amount of RANKL was dissolved in warmed medium according to the manufacturer's instructions, mixed well, and then added to the cells that had their old medium aspirated. For vehicle control, the same volume of sterile distilled water was used instead.

Statistical analysis

All data are shown as means alone or means ± SEM. Differences between two groups were analyzed using Student's *t*-test, while differences between three or more groups were analyzed using one-way ANOVA followed by Tukey's post-hoc test. *P* values of less than 0.05 were considered to be statistically significant. Differences are not statistically significant unless otherwise indicated. All statistical analyses were performed using GraphPad Prism 5 software.

5. RESULTS

5.1. Effects of EPA on aneurysmal tissue remodeling

Baseline mice characteristics were mostly not significantly different amongst the experimental groups

In order to investigate the effects of EPA on murine $CaCl_2$-induced AAAs, I designed the study with three experimental groups: (1) **Sham group** that received periaortic NaCl application (instead of $CaCl_2$) and were fed the control diet, (2) **Control diet group** that received periaortic $CaCl_2$ application and were fed the control diet, and (3) **EPA diet group** that received periaortic $CaCl_2$ application and were fed the EPA-supplemented diet. The preparation of the diets has been described in detail in the Materials and Methods section. The experimental protocol is outlined in Figure 1.

Prior to performing study analyses, I first had to (1) confirm the baseline characteristics of mice after they have received control or EPA-supplemented diets and (2) confirm the surgical procedure for inducing AAA formation in mice with periaortic $CaCl_2$ application.

As EPA is a fatty acid, there was a possibility that the EPA-supplemented diet could cause differences in the body weight of the mice between the Control diet and

EPA diet groups after AAA surgery, which may affect the interpretation of results. In addition, whether there were any differences in the amount of chow consumed between the two groups also needed to be confirmed. To this end, I assessed these baseline characteristics in the mice by recording their body weights on a weekly basis for 6 weeks as well as the amount of chow consumed daily. Interestingly, the results showed that mice fed with an EPA diet had gradual increases in body weight over 6 weeks despite having received AAA surgery, whereas the Sham and Control diet groups had an acute decrease in body weight at 1 week after AAA surgery but then recovered from Week 2 onwards to a level that was not significantly different to the EPA diet group (Figure 2A).

Consistent with the body weight data, there was also no significant difference in the mean daily amount of chow consumed between the two experimental groups (Figure 2B).

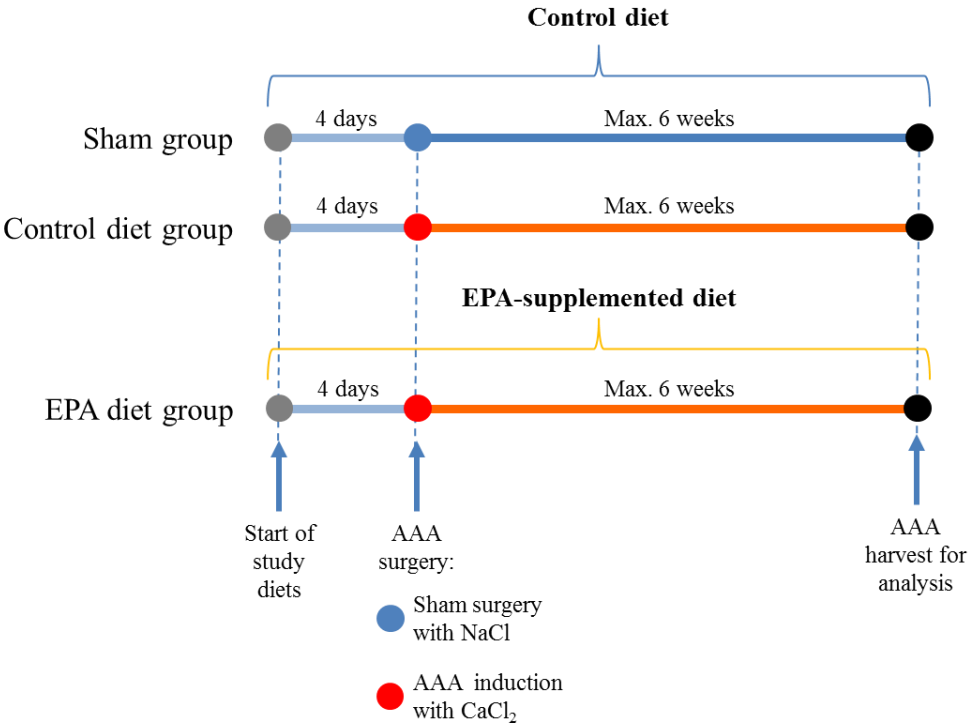

Figure 1. Study protocol. Mice in the Sham, Control diet, and EPA diet groups began receiving the indicated study diets 4 days prior to AAA surgery. Sham group received sham surgery with NaCl periaortic application, and served as a baseline group for future comparisons and analyses. Control diet and EPA diet groups received $CaCl_2$ periaortic application to induce AAA formation. The respective study diets were continued for the duration of the study. Mice were kept for a maximum of 6 weeks after surgery until sacrifice for analysis.

A

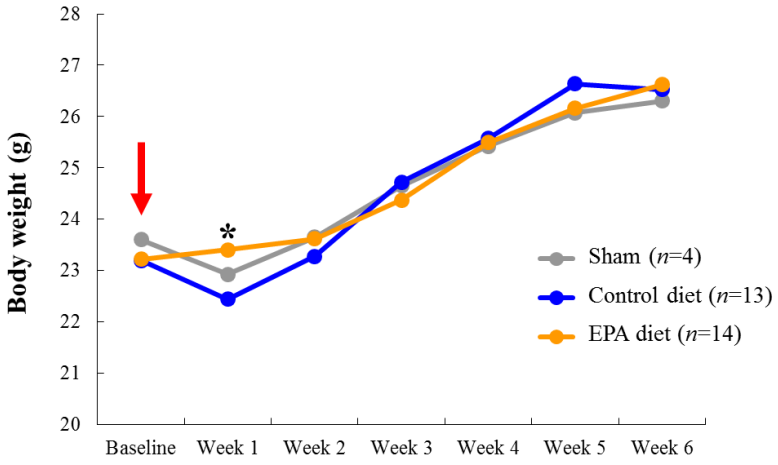

B

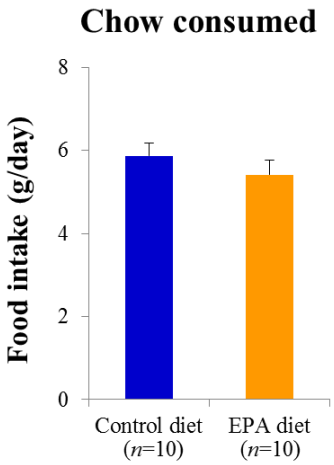

Figure 2. Baseline effects of EPA on mice in the $CaCl_2$-induced AAA model. **A.** Body weights of mice in the Sham, Control diet, and EPA diet groups were recorded weekly after AAA surgery (NaCl or $CaCl_2$ application) was performed, as indicated by the red arrow. Sham and Control diet groups received control-diet while EPA diet group received an EPA-supplemented diet. *$P < 0.05$, EPA diet group versus the Control diet group. **B.** Mean daily amounts of chow consumed by mice at baseline (prior to AAA surgery) in the Control diet and EPA diet groups. No significant differences were detected.

EPA treatment attenuates $CaCl_2$-induced AAA formation and elastic lamina destruction

Next, I investigated the effects of EPA on AAA formation. Marked dilatation and calcification of the aorta in the Control diet group was clearly visible macroscopically 6-weeks after $CaCl_2$ was applied to the infra-renal abdominal aorta; in contrast, the aortas of the mice on the EPA-supplemented diet were dilated significantly less than those of mice in the Control diet group (Figure 3A). The aortic diameters in the Control diet group were shown to have increased to approximately 1.6 times that of the aortic diameter of Sham group mice, therefore meeting the definition for aneurysm formation (≥1.5 time increase in aortic diameter [34]). In contrast, the diameter of aortas in the EPA group was only increased by approximately 1.3 times, and furthermore this increase was not statistically significant. This therefore indicates that EPA treatment attenuated the formation of $CaCl_2$-induced AAA (Figure 3B).

In order to assess the condition of the elastic fibers in the aortic wall, I performed histological staining using the Elastic van Gieson (EVG) stain. EVG staining is a well-established method for the visualization of arterial wall elastic lamina, and is one of the most commonly used stains in the assessment of AAA histology. Histological examination of EVG-stained AAAs demonstrated that the extensive matrix and elastic

lamina destruction seen in Control diet group AAAs was greatly suppressed in aortas from the EPA diet group (Figure 4). Higher magnification views showed that elastic lamina strand breaks, a hall-mark feature of AAAs, are clearly seen in AAAs of the Control diet group but were relatively absent in the EPA diet group. Taken together, these results support the notion that EPA attenuates aortic dilatation via the suppression of elastic lamina degradation, leading to the attenuation of vascular wall tissue remodeling.

A

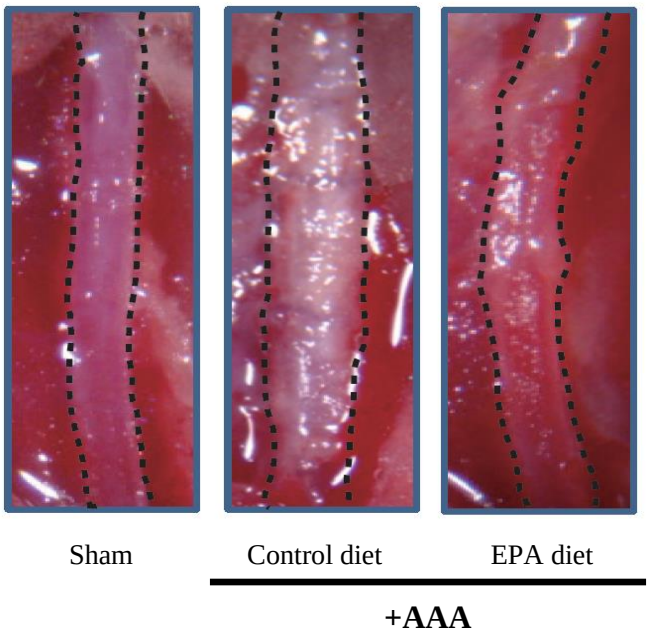

B

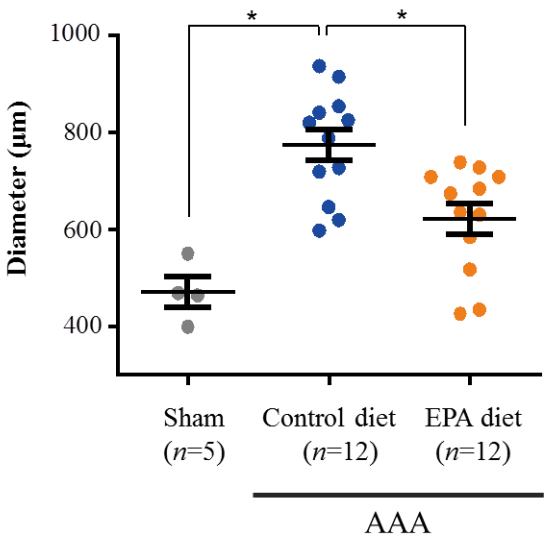

Figure 3. EPA attenuated aortic dilatation after $CaCl_2$-induced AAA surgery. A. Macroscopic appearances of *in situ* infra-renal aortas (demarcated by the black broken lines) at 6-weeks after AAA surgery, showing a much less dilated infra-renal aorta in mice that received an EPA-supplemented diet compared to the Control diet

group. Mice in the Sham group received sham AAA surgery (periaortic application of NaCl) and served as a baseline for calculations of fold-change in aortic diameter for the other two groups. Representative images of at least three independent experiments are shown. **B.** Quantitative analysis of the maximal external aortic diameters of aortas at 6-weeks after AAA surgery. *$P < 0.05$, NS, non-significant.

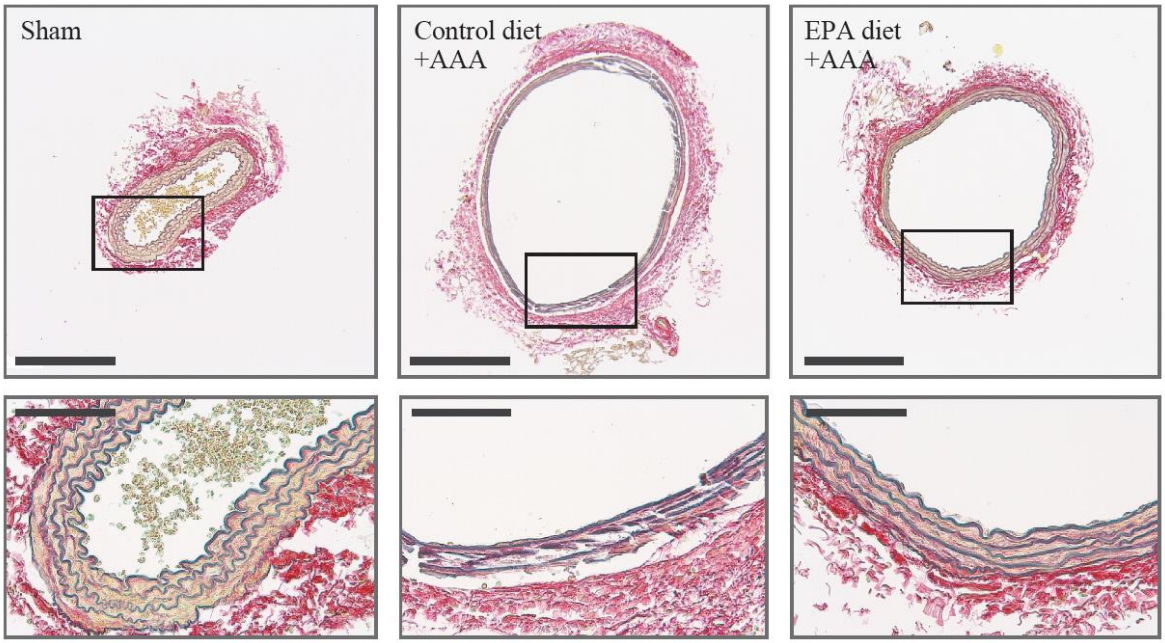

Figure 4. Administration of EPA preserves vascular wall structure in AAAs. Histological analysis by Elastica van Gieson staining, showing preserved aortic wall structure and less elastic lamina strand breaks in the aorta of mice from the EPA diet group compared to the Control diet group. Scale bars: 200 μm (upper panels) and 50 μm (lower panels). Representative images of at least three independent experiments are shown.

EPA attenuated the $CaCl_2$-induced up-regulation of MMPs but did not affect the expression levels of TIMPs or other extracellular matrix components

Given this phenotype, I subsequently began to elucidate the molecular mechanism underlying how EPA suppressed AAA formation. I first focused on examining the mRNA expression of a set of genes related to tissue remodeling such as MMPs and TIMPs. Among the genes analyzed by real-time PCR, the expression levels of *Mmp2* and *Mmp9* were significantly increased in the aortas of mice in the Control diet group at 1- and 3-weeks after $CaCl_2$ application, consistent with previous reports [19,21,25]. In contrast, mice in the EPA diet group had significantly lower levels of *Mmp2* and *Mmp9* expression (Table 2). This suggests that because of the lower expression levels of the MMPs critical to AAA formation, *Mmp2* and *Mmp9*, the tissue milieu in AAAs of mice in the EPA diet group may have been less proteolytic compared to that of the Control diet group, thereby leading to less tissue destruction.

However, considering that the balance between proteolysis and anti-proteolysis is determined by the levels of MMPs versus TIMPs, the levels of TIMPs also needed to be evaluated so as to conclude that EPA does indeed reduce the proteolytic environment of AAAs via the suppression of MMP up-regulation. To this end, the expression levels of the major TIMPs, *Timp1* and *Timp2*, was also assessed by real-time PCR. The results

showed that while the levels of TIMPs were also upregulated by the $CaCl_2$ treatment, EPA did not affect their expressions (Table 2).

Major changes in the components of the aortic wall extracellular matrix (ECM) occur as a result of the significant tissue remodeling that is invariably associated with AAA development. Therefore, I investigated whether or not EPA also had some effects on these ECM components. Since collagen I, III, and fibronectin are known to be major constituents of the aortic wall ECM [3,53], the expression levels of these factors in $CaCl_2$-induced AAAs at 1- and 3-weeks after surgery were assessed by real-time PCR. The results showed that while the expression of all three ECM components did indeed increase during AAA development compared to the Sham group, there was no significant difference between the Control diet and EPA diet groups (Table 2). These results indicate that in terms of tissue remodeling, the effects of EPA in attenuating AAA formation is most likely exerted through its suppression of MMP up-regulation rather than modulation of ECM components, resulting in a less proteolytic AAA tissue environment and less vascular wall degradation.

Table 2. Gene expression profile in 1-week AAAs analyzed by quantitative real-time PCR.

Gene	**1-week**			**3-weeks**		
	Sham (*n*=5)	**Control diet (*n*=11)**	**EPA diet (*n*=10)**	**Sham (*n*=6)**	**Control diet (*n*=11)**	**EPA diet (*n*=13)**
Ccl2	1.0±0.51	8.6±1.06	**17.8±3.69** $^{\#}$*	1.2±0.14	4.2±0.32 $^{\#}$	5.8±0.72 $^{\#}$
Col1a1	1.0±0.10	1.5±0.07 $^{\#}$	1.3±0.11	0.7±0.09	2.0±0.14 $^{\#}$	1.8±0.10 $^{\#}$
Col3a1	1.0±0.11	2.0±0.11 $^{\#}$	1.7±0.15 $^{\#}$	0.8±0.08	2.1±0.15 $^{\#}$	2.2±0.10 $^{\#}$
Fn1	1.0±0.06	8.4±0.96 $^{\#}$	10.1±0.98 $^{\#}$	1.0±0.13	2.1±0.27 $^{\#}$	2.9±0.70
Mmp2	1.0±0.11	1.8±0.07 $^{\#}$	**1.3±0.10** *	1.6±0.18	4.2±0.27 $^{\#}$	**3.5±0.17** $^{\#}$*
Mmp9	1.0±0.30	36.3±8.84 $^{\#}$	**10.6±2.11** $^{\#}$*	2.3±0.55	10.0±1.31 $^{\#}$	**4.6±0.47** *
Timp1	1.0±0.14	9.1±0.98 $^{\#}$	8.5±0.98 $^{\#}$	0.8±0.12	4.2±0.38 $^{\#}$	3.4±0.44 $^{\#}$
Timp2	1.0±0.04	0.9±0.04	0.9±0.03	1.2±0.10	1.6±0.07 $^{\#}$	1.8±0.07 $^{\#}$
Opg	1.0±0.05	1.0±0.12	**1.5±0.11** $^{\#}$*	1.2±0.16	1.6±0.14	2.2±0.33 $^{\#}$
Rankl	1.0±0.41	29.2±4.38 $^{\#}$	**14.1±2.64** *	2.5±0.55	14.2±1.12 $^{\#}$	**7.6±0.96** $^{\#}$*
Runx2	1.0±0.07	4.3±0.29 $^{\#}$	3.9±0.41 $^{\#}$	1.0±0.18	5.8±0.43 $^{\#}$	4.5±0.43 $^{\#}$

Messenger RNA levels of major MMPs associated with AAA formation, ECM components, and vascular calcification factors in infra-renal aortas at 1- and 3-weeks after AAA surgery were analyzed using real-time PCR. All expression levels were first normalized to *18s* rRNA levels (house-keeping gene) and then presented as fold change over the Sham group value at 1-week. Results are mean ± SEM. $^{\#}P < 0.05$ vs. Sham group of the same time-point; $*P < 0.05$ vs. Control diet group of the same time-point (further indicated in bold-type), one-way ANOVA with Tukey's post-hoc test.

.

In order to confirm the decrease in MMP levels in AAAs by another method, I performed zymography using 1-week AAA samples. Gelatin zymography is a well-established technique to detect the functional activity of MMPs present in tissues or cells [50]. To detect the activities of MMP-2 and MMP-9, the two MMPs that appeared to be affected by EPA based on the real-time PCR results (Table 2), a gelatin gel was chosen because gelatin is a substrate that can be degraded by these two MMPs. Consistent with the results of real-time PCR, zymography showed that the functional activities of pro-MMP-2, cleaved MMP-2, and MMP-9 were indeed all markedly decreased in the EPA diet group compared to the Control diet group, suggesting that the reduced mRNA levels of *Mmp2* and *Mmp9* translated to a significant difference in their functional activities at the protein level in the AAA tissues as well (Figure 5A, B).

A

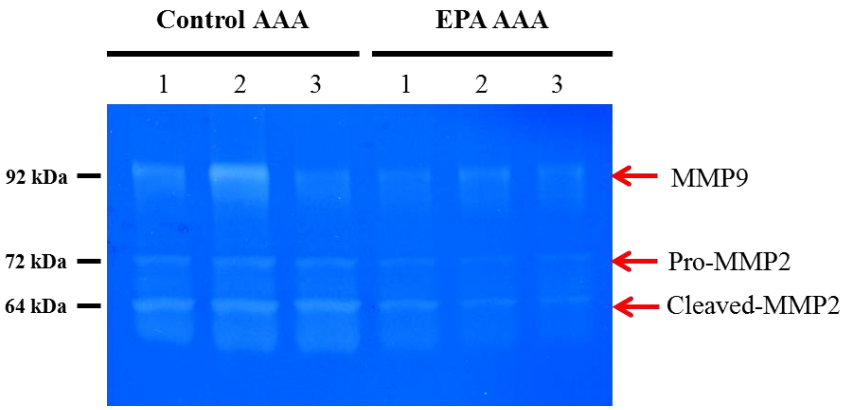

B

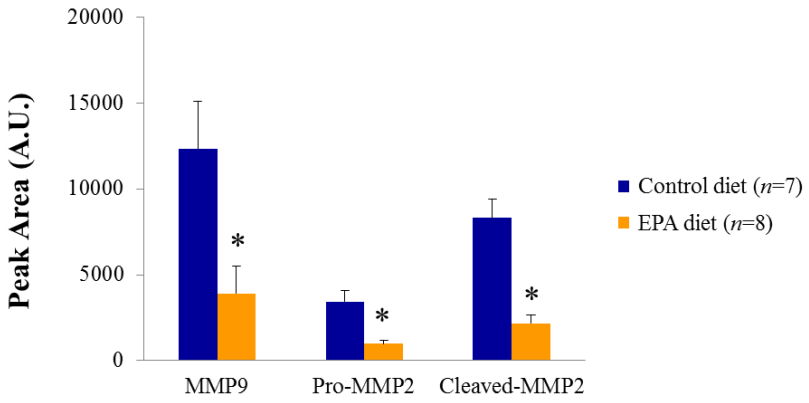

Figure 5. Reduced functional activities of MMP-2 and MMP-9 in AAAs after EPA treatment. A. Representative gelatin zymography gel showing reduced activities of the proform of MMP-2 (pro-MMP2), cleaved form of MMP-2 (cleaved-MMP2), and MMP-9 in 1-week AAA samples after EPA-feeding compared to the AAAs of the Control diet group. Each lane represents a separate AAA sample within the same treatment group. Equal amount of protein (20 μg) was loaded per AAA sample. kDa, kilodalton. **B.** Quantitative analysis of zymographic MMP activities. Data are mean ± SEM of three independent experiments. *$P < 0.05$ versus Control diet group.

EPA suppresses Mmp9 expression in AAA macrophages

Previous reports have demonstrated that *Mmp9*-deficient mice are resistant to experimental AAA formation [16,25]. Given that EPA seemed to impart a greater effect on *Mmp9* expression than on *Mmp2*, I decided to analyze specifically how EPA suppresses MMP-9 activity in AAAs. Macrophages have been reported to be the major producer of MMP-9 in AAA tissues [22,25,54]. Therefore, there were at least two possible mechanisms by which EPA could have suppressed MMP-9 levels in the AAA: (1) reducing the number of macrophages recruited to the AAAs, and (2) suppressing the ability of macrophages to produce MMP-9.

Flow cytometry was used to test these two hypotheses. Since the number of macrophages recruited to the AAA could be affected by the number of available circulating monocytes as well as the level of chemoattractant cytokine, i.e. CCL2, expressed by the AAA to recruit monocytes, I proceeded to investigate the number of circulating monocytes, the number of macrophages in the AAAs, and the expression level of *Ccl2* in the AAAs of the Control diet and EPA diet groups. However, before performing these analyses, the gating strategy for isolating macrophages needed to be confirmed from a technical perspective. The cell surface markers of circulating monocytes are well established and can be easily identified by gating for Ly-6G$^-$ cells

(to exclude granulocytes such as neutrophils) that are $CD11b^{+}$ and Ly-$6C^{hi}$ in the peripheral blood (Figure 6) [29,55]. Meanwhile in the AAA tissue, by first gating for Ly-$6G^{-}$ cells from the dissociated AAA cells, macrophages could subsequently be identified as Ly-$6C^{low}CD11b^{+}F4/80^{+}$ cells (Figure 7A, B) [32]. These macrophages were isolated by fluorescence-activated cell sorting (FACS), and their cellular appearance was shown to be consistent with that of typical macrophages (Figure 7C).

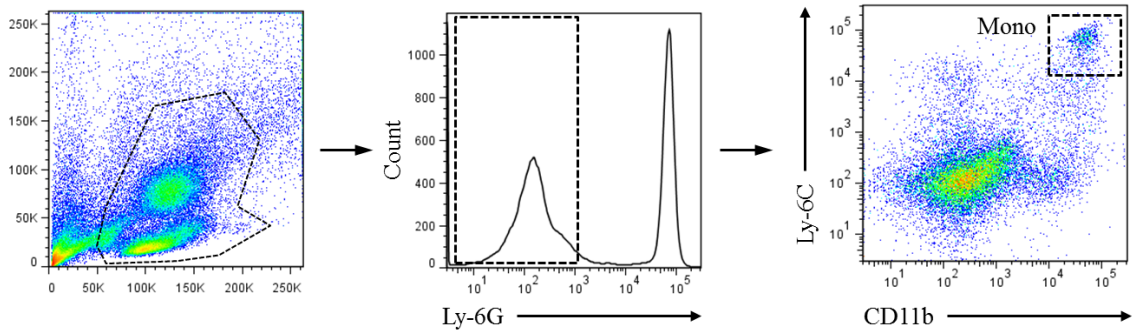

Figure 6. Gating strategy for the flow cytometric analysis of peripheral circulating monocytes. Representative flow cytometric plots of peripheral blood analysis are shown. Living cells isolated from the peripheral blood of mice at 1-week after AAA surgery were first gated on Ly-6G (granulocyte marker), and Ly-6G^{-} cells were further analyzed for expression of the myeloid markers Ly-6C and CD11b. Ly-6C^{hi}CD11b^{+} cells were taken to be monocytes according to previous reports [29,55].

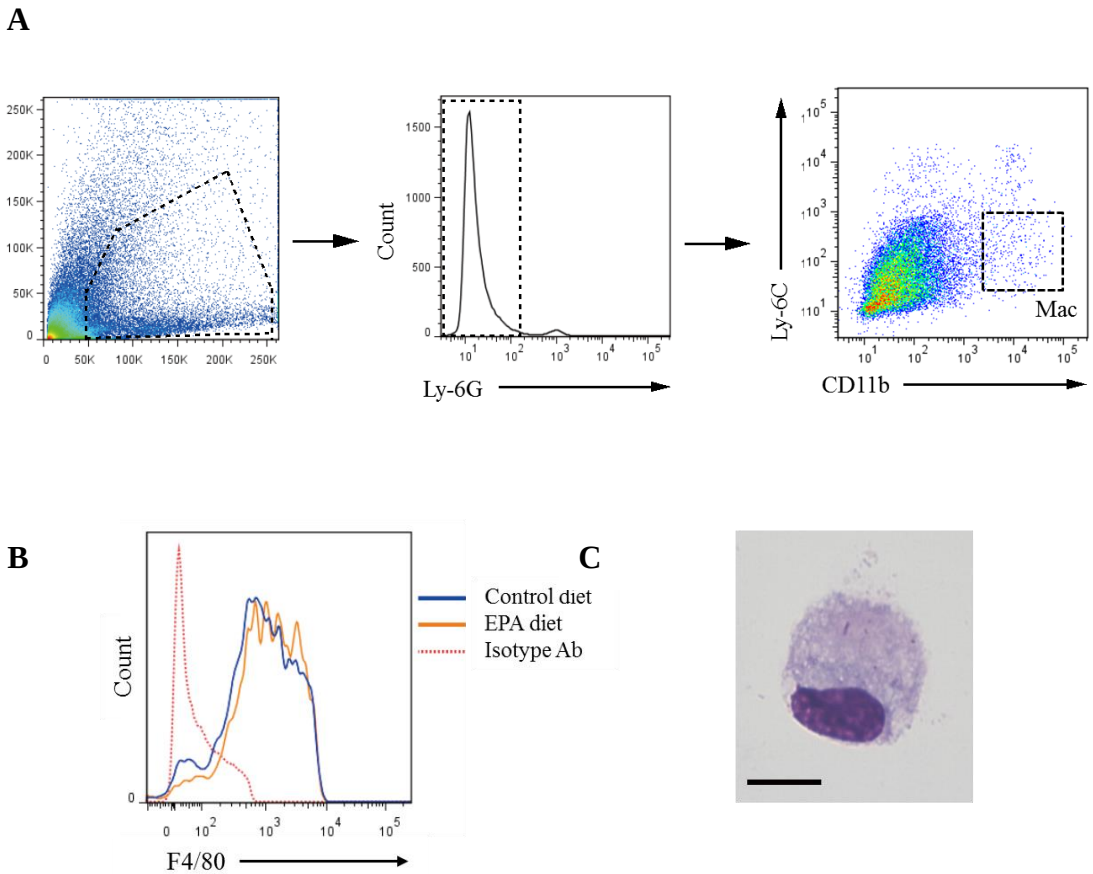

Figure 7. Gating strategy for the flow cytometric analysis of AAA macrophages. Representative flow cytometric plots of AAA analysis are shown. Similar to the gating strategy for the peripheral blood analysis, living cells isolated from AAA tissues 1-week after the AAA surgery were first gated on Ly-6G, and Ly-6G^{-} cells were further analyzed for expression of Ly-6C and CD11b **(A)**; Ly-6C^{low}CD11b^{+} cells were shown to be positive for F4/80, a macrophage marker **(B)**, and together Ly-6C^{low}CD11b^{+}F4/80^{+} cells were taken to be aneurysmal macrophages and used in all subsequent analyses. **C.** Giemsa staining of sorted Ly-6C^{low}CD11b^{+}F4/80^{+} cells from the aorta shows cells with the characteristic macrophage appearance. Scale bar, 10 μm.

Using these gating strategies to test my first hypothesis, I proceeded to assess the number of monocytes in peripheral blood and the number of macrophages in AAAs at 1-week after the surgery in the Control diet and EPA diet groups. Surprisingly, while the difference in the number of circulating Ly-6C^{hi}CD11b^{+} monocytes was not statistically significant, mice treated with EPA tended to have higher numbers of circulating monocytes (Figure 8). In addition, when I examined the tissue mRNA expression levels of *Ccl2* in the AAAs at the same time-point of 1-week after AAA surgery, aortas of mice in the EPA diet group had significantly higher *Ccl2* expression than the aortas of mice in the Control diet group (Table 2). These two results together should have suggested more potent recruitment of circulating monocytes to AAAs by CCL2 in the EPA diet group, leading to the presence of more macrophages in the AAA and which would be completely contrary to the initial hypothesis. However, upon examining the actual number of macrophages in the AAA amongst the Control diet and EPA diet groups, there was interestingly no statistically significant difference in the number of aneurysmal Ly-6C^{low}CD11b^{+}F4/80^{+} macrophages between the Control diet and EPA diet groups (Figure 9). This indicates that despite the higher potential for monocyte recruitment to AAAs in the EPA diet group, EPA suppressed the actual recruitment and/or infiltration of monocytes.

To test the second hypothesis, I sorted the AAA macrophages from both groups at 1-week after AAA surgery and examined their *Mmp9* mRNA expression by real-time PCR. The results showed that there was significantly less *Mmp9* expressed by macrophages sorted from the AAAs of mice in the EPA diet group (Figure 10), suggesting that EPA directly affected macrophage function, such as MMP production, within the AAA tissue while AAA macrophage numbers were unaffected. The combination of no difference in macrophage numbers and an absolute decrease in macrophage-derived MMP-9 levels in the AAAs of the EPA diet group resulted in a net fall in total MMP-9 levels and activity, thereby helping to explain the reduced MMP-9 activity and gene expression in whole AAA samples as well as the attenuation of AAA formation.

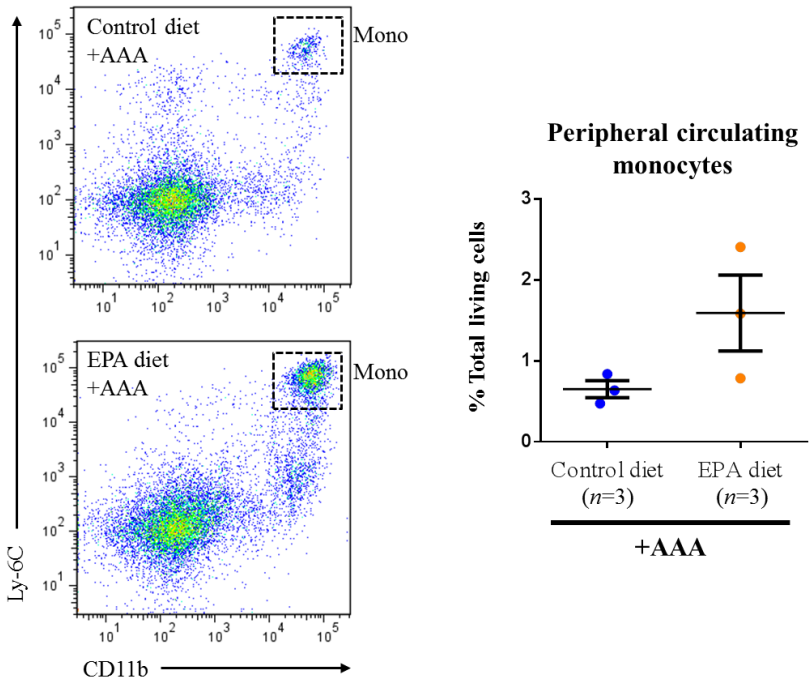

Figure 8. EPA tends to increase circulating monocyte numbers at 1-week after AAA surgery. Representative flow cytometric plots of circulating monocytes in peripheral blood of mice in the Control diet and EPA diet groups at 1-week after the AAA surgery, gated by the myeloid cell markers Ly-6C and CD11b. After the blood was sampled via cardiac puncture, the mice were sacrificed and aortas were harvested for subsequent flow cytometric and mRNA expression analyses. While the difference in the number of $CD11b^{+}Ly\text{-}6C^{hi}$ circulating monocytes was not statistically significant between the two groups (P = 0.1213 by unpaired Student's t-test), EPA tended to increase the number of monocytes.

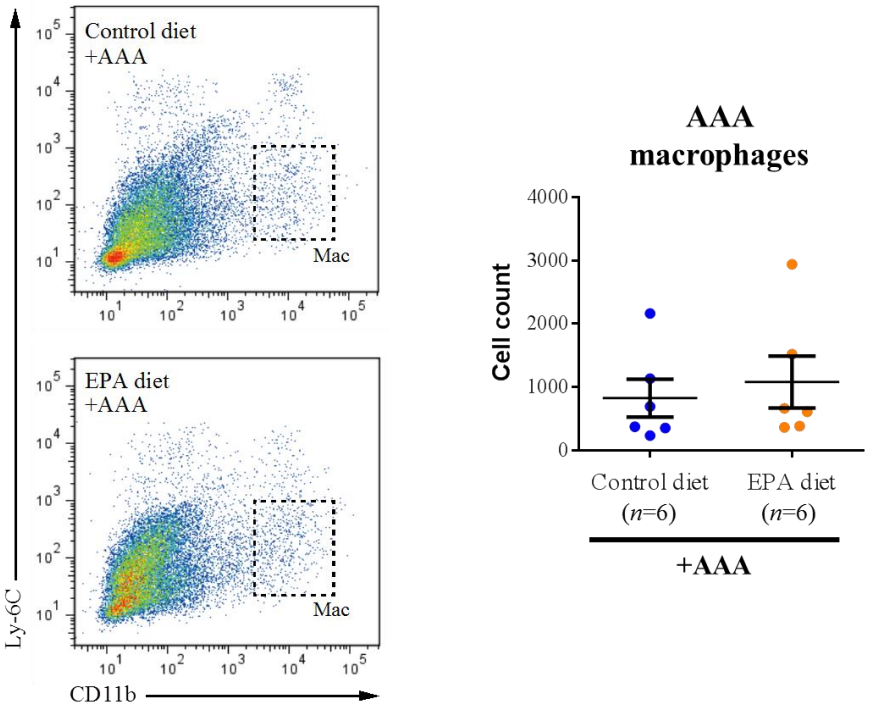

Figure 9. AAA macrophage numbers are not significantly different between the Control diet and EPA diet groups. Representative flow cytometric plots of AAA macrophages from mice in the Control diet and EPA diet groups at 1-week after the AAA surgery, gated by the myeloid cell markers Ly-6C and CD11b. Three AAAs from each group were pooled into one sample in each experiment. Quantifying the mean number of Ly-6C^{low}CD11b^{+}F4/80^{+} aneurysmal macrophages per AAA sample showed that there was no statistically significant difference between the two groups. Data are mean ± SEM of six independent experiments.

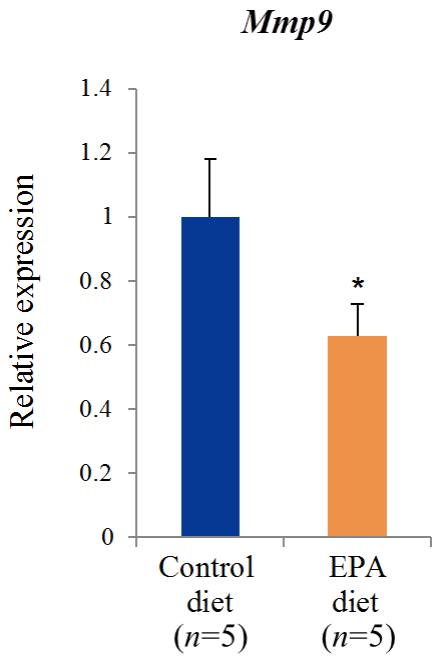

Figure 10. mRNA levels of *Mmp9* in sorted AAA macrophages. Macrophages from AAAs in the Control diet and EPA diet groups at 1-week after AAA surgery were sorted and their *Mmp9* expression levels were analyzed by real-time PCR. Expression levels were first normalized to *18s* rRNA levels and then expressed as the relative expression to the level of Control diet group. Three AAAs from each group were pooled into one sample in each experiment. Data are mean ± SEM of five independent experiments. *$P < 0.05$ compared to the Control diet group.

Macrophage expression of Mmp9 is directly suppressed by EPA

Given the *in vivo* results, the next question was whether EPA would have the same effect *in vitro* and suppress *Mmp9* expression in cultured macrophages. To address this possibility, I used the well-established RAW264.7 macrophage cell line and treated these cells with EPA *in vitro* with or without TNF-α stimulation to induce *Mmp9* expression.

Firstly, the results showed that TNF-α effectively induced *Mmp9* expression in RAW264.7 macrophages, as can be seen by the more than two-fold increase in *Mmp9* expression in the vehicle control group after TNF-α stimulation (Figure 11). When RAW264.7 macrophages were treated with increasing concentrations of EPA, there was a dose-dependent reduction in the expression of *Mmp9* at both baseline and after TNF-α stimulation, although the effects at baseline were small and non-significant (Figure 11). This lends strong support to the direct effects of EPA on macrophage *Mmp9* expression. Taken together with the previous *in vivo* results, it appears that EPA directly affects macrophages to reduce their *Mmp9* expression in both *in vivo* and *in vitro* conditions.

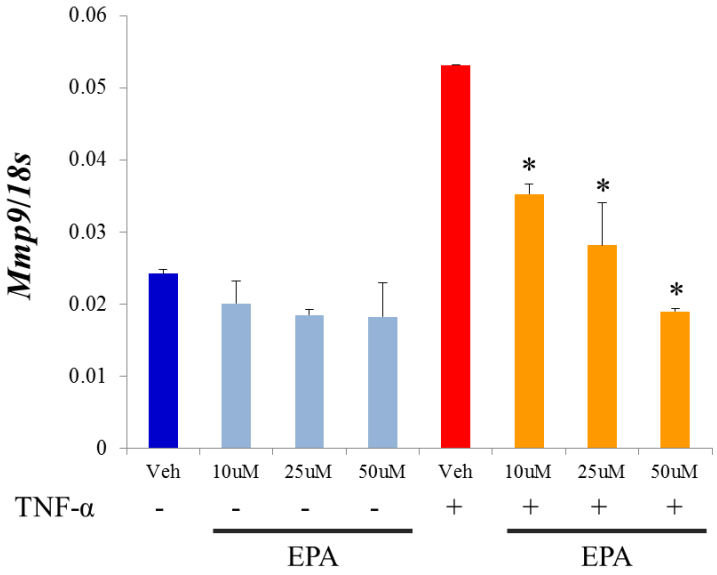

Figure 11. EPA dose-dependently suppresses macrophage *Mmp9* expression *in vitro*. RAW264.7 macrophages were cultured with either vehicle (10% BSA) or EPA (10, 25, or 50 μmol/L) for 48 hours. The cells were then stimulated with TNF-α (20 ng/mL) for a further 6 hours and harvested for analysis by real-time PCR. Expression levels were normalized to *18s* rRNA levels. *n*=3 per condition. Results are mean ± SEM. **P* < 0.05 compared to the vehicle control after TNF-α stimulation.

5.2. Effects of EPA on vascular calcification in the aneurysm

Aortic calcification was suppressed by EPA

In a separate, interesting finding, I found that the aortic walls of $CaCl_2$-induced AAAs in BALB/cA mice from the Control diet group had clear, macroscopically visible calcification (Figure 3A). This calcification was not as evident when another strain of mouse (C57BL/6j) was used (data not shown), suggesting the existence of strain-specific differences in vascular calcification in response to $CaCl_2$ treatment that have not yet been reported. In BALB/cA mice, I found that an EPA-supplemented diet markedly attenuated this vascular calcification compared to AAAs in the Control diet group, which was visible macroscopically (Figure 3A). To investigate this further, I imaged mice in the Sham, Control diet and EPA diet groups at 6-weeks after AAA surgery with micro-computed tomography (CT) and confirmed that the volume of calcification along the area of the aorta to which $CaCl_2$ had been applied was significantly reduced in the EPA diet group compared to the Control diet group (Figure 12).

Given the reduction in vascular calcification by the EPA-supplemented diet, I next examined the expression levels of factors known to be implicated in this process. *Runx2* (a master regulator of vascular calcification), *Rankl* (encoded by *Tnfsf11*, shown

to be a major effector molecule mediating vascular calcification downstream of RUNX2), and *Opg* (encoded by *Tnfrsf11b*, a factor that binds to RANKL to block its actions by acting as a decoy receptor and inhibit vascular calcification) are three major factors known to be critically involved in vascular calcification [39-41]. A marked up-regulation of *Runx2* and *Rankl* was observed in AAAs of the Control diet group at 1- and 3-weeks after $CaCl_2$-induction (Table 2), suggesting the close involvement of these factors in the calcification seen in $CaCl_2$-induced AAAs and consistent with previous reports of their roles in vascular calcification. Interestingly, an EPA-supplemented diet significantly attenuated *Rankl* up-regulation while it significantly increased the expression of its inhibitor *Opg* at 1-week after AAA surgery. Meanwhile, there were no differences in the expression of *Runx2* between the Control diet and EPA diet groups, indicating that EPA may be suppressing *Rankl* expression somewhere downstream of RUNX2-mediated pathway in addition to other pathways. Taken together, these results suggest that the combination of (1) the reduction in levels of calcification-promoting *Rankl* and (2) increased levels of the calcification-inhibiting *Opg* may explain why vascular calcification was suppressed in the AAAs of mice fed an EPA-supplemented diet.

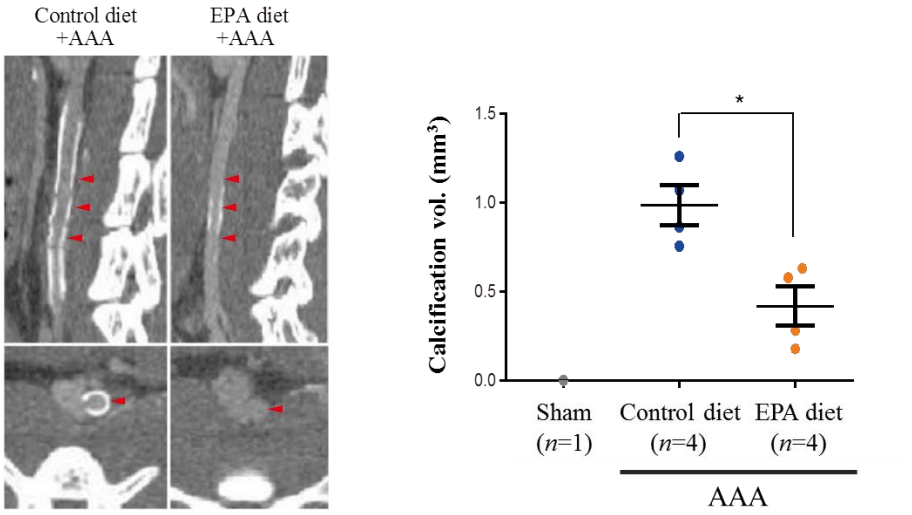

Figure 12. $CaCl_2$-induced AAAs form clear vascular calcification, and this is ameliorated by EPA. Aortic calcification was assessed by micro-CT imaging of *in situ* aortas 6-weeks after perivascular $CaCl_2$ application. Both sagittal and transverse slices show reduced overall calcification in the AAAs from the EPA diet group compared to the Control diet group, and this was consistent with the results of quantitative analysis of the total calcification volume in each aorta. Red arrowheads indicate the infra-renal aorta. Representative images of two independent experiments are shown. *$P < 0.05$ compared to Control diet group.

Given the fact that EPA concurrently reduced both vascular calcification and tissue remodeling in the AAA, the next interesting question was whether these two processes were in fact related to each other. I hypothesized that the factors involved in vascular calcification - in particular, *Rankl* - may contribute to both vascular calcification as well as tissue remodeling processes by inducing MMP production in macrophages. To test this idea, I tested whether RANKL protein could induce *Mmp9* expression in cultured macrophages. Using previously reported protocols involving RANKL stimulation of macrophages and other similar cells [56], I treated peritoneal macrophages with RANKL to test the response in cultured macrophages. Peritoneal macrophages clearly showed a time-dependent up-regulation of *Mmp9* in response to RANKL, with expression levels of *Mmp9* being approximately 3-fold that of the respective control at 3 days after stimulation (Figure 13).

The *in vitro* results indicate that RANKL has the potential to induce *Mmp9* up-regulation in macrophages. This suggests that it may be possible for RANKL to act as an activator *in vivo* to stimulate AAA macrophages to produce MMP-9, and therefore partially contribute to tissue remodeling and aortic dilatation. To assess this possibility, I investigated whether *Mmp9* expression was associated with *Rankl* expression in the AAAs to support their causal relationship. Since *Mmp9* expression seems to be highest

at 1-week of the time-points analyzed (Table 2), I assessed the expressions of *Mmp9* and *Rankl* in the AAAs of wild-type mice within 1 week after AAA surgery (at 1, 3, and 5 days). The results show that *Rankl* expression increased rapidly within a day of AAA surgery, with the increasing trend maintained at 3 and 5 days (Figure 14). Most importantly, *Mmp9* expression was similarly up-regulated during the time period analyzed, albeit with a slower starting increase. This supports the notion that with increasing *Rankl* expression in the aorta soon after AAA surgery, the RANKL protein becomes more available and abundant to act as an activator of macrophages in AAAs to contribute to *Mmp9* expression up-regulation and subsequent tissue-remodeling.

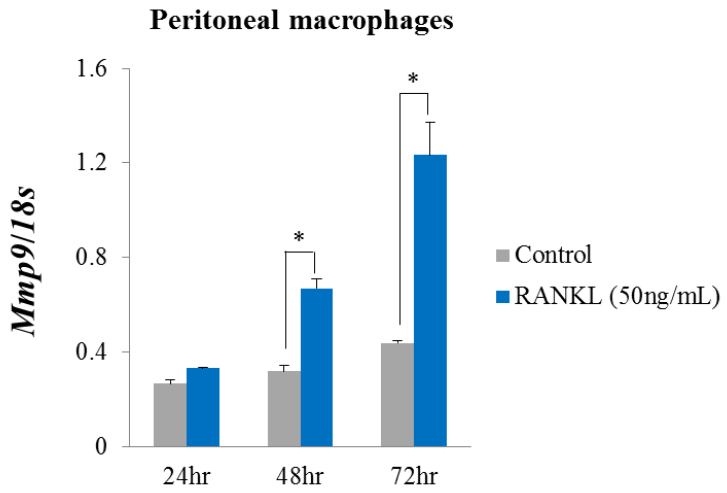

Figure 13. RANKL (TNFSF11) up-regulated *Mmp9* expression in peritoneal macrophages. Thioglycollate-elicited peritoneal macrophages from wild-type BALB/cA mice were stimulated with recombinant mouse RANKL protein (50 ng/mL) and time-course analysis of *Mmp9* expression over 72 hours was performed. All gene expression levels were normalized to *18s* rRNA levels. *n*=3 per group at each time-point. Data are mean ± SEM and representative of 3 independent experiments. **P* < 0.05.

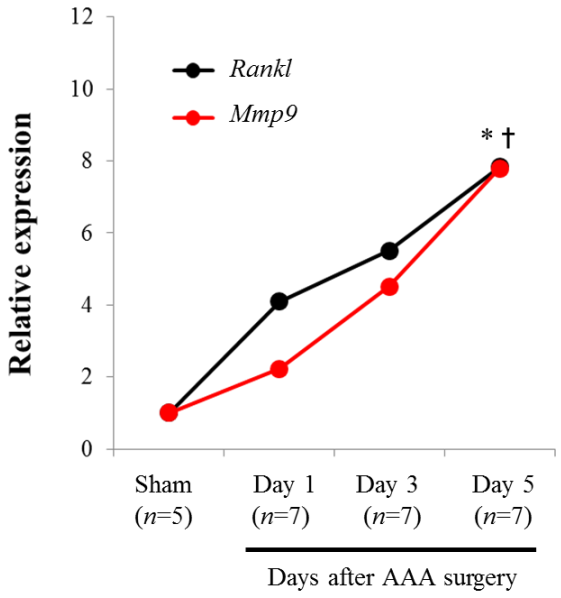

Figure 14. Levels of *Mmp9* and *Rankl* both increase during the early phases of AAA formation. The mRNA levels of *Mmp9* and *Rankl* in the early phase of AAA formation (1 to 5 days after perivascular $CaCl_2$ application) in wild-type BALB/cA mice were analyzed using real-time PCR. Gene expression levels were first normalized to *18s* rRNA levels and then presented as relative expression to the Sham group. The results showed a positive correlation between increasing *Rankl* and *Mmp9* mRNA levels. Data are mean of 3 independent experiments. *$P < 0.05$ compared to Sham group for *Mmp9*, † $P < 0.05$ compared to Sham group for *Rankl*.

The mechanism by which EPA attenuates *Rankl* up-regulation can be two-fold: (1) reduce total *Rankl* gene expression in AAAs so that induction of AAA macrophage *Mmp9* expression is decreased, and (2) directly inhibiting the action of RANKL on macrophages. The first mechanism has been shown to be true since the results showed that *Rankl* expression at 1-week after AAA surgery was markedly less in the AAAs of the EPA diet group than the Control diet group (Table 2). To test whether the second mechanism was also true, I treated peritoneal macrophages *in vitro* with EPA and recombinant mouse RANKL protein and analyzed the expression of *Mmp9* after 72 hours of stimulation. This experiment showed that while EPA had a slight tendency to reduce RANKL-induced *Mmp9* up-regulation in peritoneal macrophages, this effect was not statistically significant (Figure 15). Taken together, these results suggest that EPA would inhibit vascular calcification and macrophage-derived MMP-9 by reducing the total amount of RANKL available in AAAs rather than by directly affecting macrophage response to RANKL.

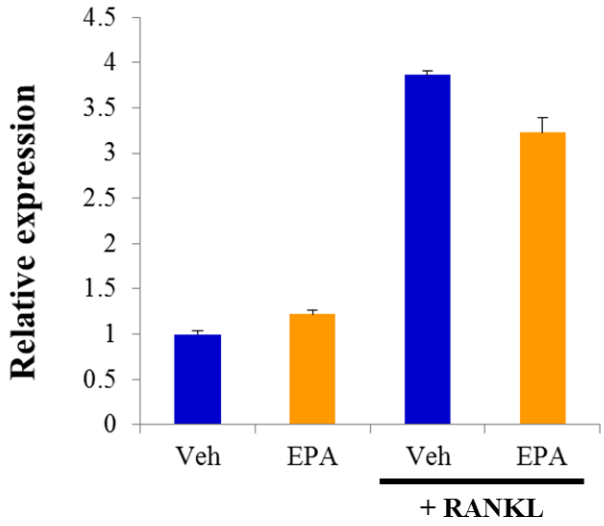

Figure 15. EPA does not significantly affect RANKL-induced up-regulation of *Mmp9*. Thioglycollate-elicited peritoneal macrophages from wild-type BALB/cA mice were treated with EPA and stimulated with RANKL (50 ng/mL) for 72 hours, after which *Mmp9* expression was analyzed. Gene expression levels were first normalized to *18s* rRNA levels and then presented as relative expression to baseline vehicle sample. *n*=3 per group for each condition. Data are mean ± SEM and representative of three independent experiments.

6. DISCUSSION

Abdominal aortic aneurysm is a prevalent disease particularly amongst elderly males and tobacco smokers that has few available pharmacological treatments [3]. In this study, I demonstrated that the ω-3 PUFA, EPA, can attenuate AAA formation in a murine $CaCl_2$-induced AAA model by suppressing AAA macrophage *Mmp9* expression. Furthermore, EPA-diet was also found to suppress vascular calcification in the model, most likely via its effects in suppressing *Rankl* up-regulation. The fact that RANKL can directly up-regulate macrophage expression of *Mmp9* suggests an additional pathway by which AAA *Mmp9* expression can be further reduced, and hints at a previously unappreciated link between vascular calcification and AAA formation (Figure 16).

In use clinically for over twenty years now, EPA alone or in combination with other ω-3 fatty acids has been shown to have pleiotropic benefits across a variety of diseases, such as the primary and secondary prevention of major coronary events [46,57], reduction of heart failure incidence [58], lowering blood pressure [59], improving outcomes of surgical and intensive care patients [60], and preserving renal function in patients with IgA nephropathy [61]. Further adding to these reports, our findings suggest that EPA may also be useful in slowing or preventing AAA formation.

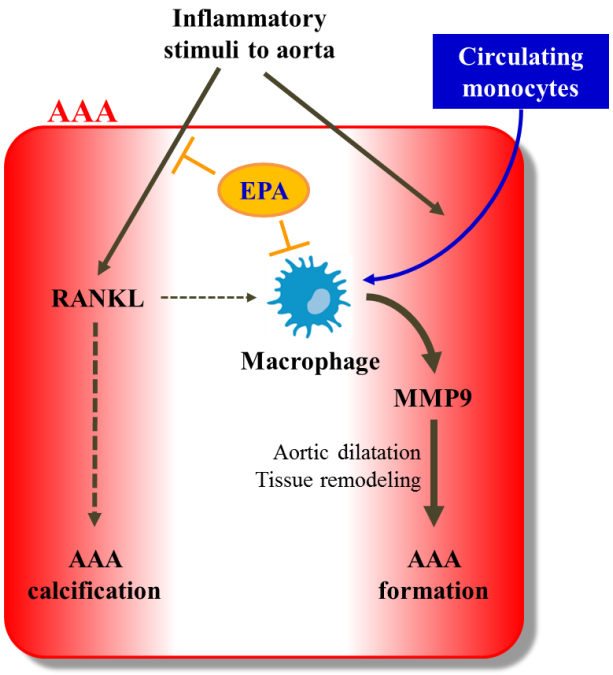

Figure 16. Schema of the mechanisms by which EPA suppresses AAA formation. This study demonstrated that EPA (1) directly suppresses AAA macrophage *Mmp9* expression, and (2) inhibits vascular calcification in the AAA by down-regulating *Rankl* expression. In addition, since RANKL was shown to induce *Mmp9* up-regulation in macrophages, reduced AAA levels of *Rankl* may also contribute to reduced macrophage *Mmp9* levels.

Our results suggest that inhibition of *Mmp2* and *Mmp9* expression is one of the potential mechanisms by which EPA modulates tissue remodeling processes during AAA formation. The expressions of *Timp1* and *Timp2*, both of which are tissue inhibitors of a wide range of MMPs including MMP-9 and MMP-2 [62,63], were not affected by EPA. Given that reduced levels of both *Timp1* and *Timp2* in AAAs have been shown to be associated with aneurysm formation as well [62,63], it is likely that administration of EPA shifted the AAA microenvironment from a pro-proteolytic to an anti-proteolytic milieu by altering the balance between MMP-9, MMP-2, and TIMP levels. The end result is reduced proteolysis with preserved anti-proteolytic activity, leading to decreased vascular wall damage and elastin degradation.

While I did not examine other immune cells such as T cells, neutrophils, or mast cells in this study, it is clear from numerous past reports that macrophages are the major cell types that produce MMP-9. In addition, in many of the reports that described the importance of other immune cells in AAA development, it is interesting to also note that concurrent decreases in macrophage numbers were also found in these studies. This further supports the concept that macrophages are one of the major final effector cells in AAA formation, where they are modulated by the cytokines produced by other immune cells that contribute to macrophage recruitment and the up-regulation of their MMP

expression. In this study, I found that there were no statistically significant differences in the number of aneurysmal macrophages between the Control diet and EPA diet groups. More surprisingly, the number of circulating monocytes was higher with EPA treatment than without, suggesting a paradoxically heightened inflammatory response in the mice that received EPA. Although these results were somewhat unexpected, it is interesting that Arnardottir *et al* [64] and Blok *et al* [65] also reported similar findings where mice treated with fish oils rich in ω-3 PUFAs had increased circulating monocytes and serum CCL2 and TNF-α compared to control mice when these animals were IP injected with lipopolysaccharide (LPS) to induce inflammation. In addition, in a report by Itoh *et al* [49], white adipose tissue from genetically obese *ob/ob* mice fed an EPA-supplemented diet also exhibited a paradoxically increased adipose tissue macrophage content despite overall improved metabolic parameters. Itoh *et al* attributed this increase in macrophage accumulation to the difference in fat intake between the EPA-treated and control groups, where EPA-treated mice received roughly twice the amount of fat compared to control mice. Given the similarities in the feeding protocol between my study and the study by Itoh *et al*, it is likely that the same mechanism may underlie my observations. Therefore, the results of my and other studies suggest that EPA as a dietary supplement can have significant immunomodulatory effects that seem

to lead to a specific heightened inflammatory response but which may not necessarily be “bad”. For example, an alternative interpretation of the increased number of circulating monocytes after EPA treatment may be that the mice have improved peripheral immune surveillance, although further studies will need to be undertaken to clarify this interpretation. Furthermore, the fact that aneurysmal macrophage numbers were not significantly different between the experimental groups despite the higher AAA *Ccl2* expression suggests that EPA partially suppressed the effect of CCL2 on monocyte recruitment. Taken together, despite the increased circulating monocyte numbers, EPA nevertheless attenuated AAA formation by qualitatively modulating macrophage function (as demonstrated by the direct suppression of macrophage *Mmp9* expression both *in vivo* and *in vitro*) while not having any significant quantitative effects on macrophage infiltration.

Although EPA did not reduce the accumulation of macrophages within AAA tissues, it suppressed macrophage *Mmp9* expression. Previous studies have shown that genetic deletion of *Mmp9* inhibits $CaCl_2$-induced AAA and that macrophages are the major source of MMP-9 in AAAs [25,54]. Moreover, EPA inhibited TNF-α-induced expression of *Mmp9* in RAW264.7 macrophages. Based on these results, it is likely that macrophages are one of the major cell-types that are directly affected by EPA in the

AAA tissue. However, the expression of *Mmp2* was also modestly but significantly decreased by an EPA-supplemented diet. In the AAA milieu, MMP-2 is considered to be primarily supplied by SMCs and fibroblasts and has also been shown in animal studies to be essential for the development of AAA [25,66]. Therefore, it appears that the effects of EPA on AAA formation may not simply be limited to macrophages. Indeed, the finding that EPA suppressed vascular calcification and *Rankl* expression in AAA suggest that EPA may also modulate the function of SMCs. This is supported by reports demonstrating the central role played by SMCs in vascular calcification and the importance of RANKL in this process [38,39,67]. Furthermore, SMC-derived RANKL has also been suggested to recruit macrophages and promote their osteoclastic differentiation [67], illustrating an important SMC/macrophage interaction via which EPA may further exert its effect when it suppresses RANKL levels in AAA. Taken together, the reduction in SMC- and fibroblast-derived MMP-2 most likely also contributed to the observed property of EPA in attenuating $CaCl_2$-induced AAA formation. Further investigations using whole-body and SMC-specific RANKL knock-out mice will help determine the exact role of vascular calcification, and RANKL in particular, in AAA formation. In addition, it may also be interesting to investigate the

use OPG as a treatment for AAAs in experimental models given its RANKL-inhibitory effects in future studies.

There are several likely mechanisms by which EPA suppresses macrophage *Mmp9* expression. Firstly, given that *Mmp9* expression is partly NFκB-dependent, one such mechanism is through the modulation of NFκB pathways by EPA. Indeed, in a study using a human keratinocyte cell line, Kim *et al* described the ability of EPA to inhibit p65 phosphorylation via p38 and Akt inhibition, thereby leading to reduced NFκB-dependent TNF-α-induced *Mmp9* expression [68]. This is supported by other studies that demonstrated that PPARα-dependent pathways and reduced IκB-α phosphorylation are also involved in the attenuation of NFκB activation [69,70]. Secondly, changes in the levels of biological eicosanoids such as prostaglandins (PGs) within the AAA as a result of EPA supplementation may also affect MMP-9 levels. Proinflammatory PGs such as PGE2 are derived from the arachidonic cascade, whereby the ω-6 PUFA arachidonic acid (AA) is metabolized by a series of enzymes that include cyclooxygenase (COX)-2 and prostanoid synthases to produce a range of biologically active PGs. It is well known that EPA can compete with AA for the enzymes that catalyze PG production. Indeed, this competition is considered as one of the main beneficial effects of ω-3 PUFAs [71]. As a result of this competition, the levels of

EPA-derived anti-inflammatory PG_3 series of PGs increases while the AA-derived inflammatory PG_2 series of PGs (including PGE2) decreases, thus creating an anti-inflammatory milieu relative to the basal state without EPA supplementation [72]. Numerous studies have shown that reducing PGE2 production either by genetic deletion or pharmacological inhibition of enzymes that catalyze its synthesis can attenuate AAA formation [73-75]. There is also evidence that direct stimulation of macrophages and other cell types with PGE2 induces MMP-9 expression [76-78]. While the direct measurement of the tissue concentrations of various EPA-derived metabolites in AAA samples was beyond the scope of this study, results from the aforementioned studies together suggest that EPA may possibly also attenuate AAA formation and macrophage MMP-9 production through modulating the tissue levels of PGs (in particular PGE2).

This study has several limitations. First of all, the role of blood pressure in the effects of EPA on AAA formation was not investigated in this study. However, the effects of EPA on blood pressure have been investigated in numerous clinical trials. A meta-analysis of 31 controlled trials that involved patients who were given ω-3 fatty acid supplementation concluded that fish oil may have a small effect on blood pressure of -3.0/-1.5 mmHg (systolic/diastolic blood pressure) in hypertensive patients but not normotensive, healthy patients [79]. From these results, the authors suggest that the

blood pressure lowering effect of ω-3 fatty acids such as EPA is unlikely to be clinically significant. Meanwhile, clinical guidelines generally recommend optimal blood pressure control in the management of AAAs (especially for those with large AAAs) with agents such as β-blockers or ACE inhibitors because hypertension, treated or untreated, has been shown to be associated with later AAA development [80]. However, it is interesting to note that hypertension was not found to be a risk factor for the actual subsequent progression of AAAs in some large scale clinical trials [81], and that β-blockers or ACE inhibitors were also not shown to inhibit AAA progression [4,81]. Given these reports, the role of hypertension *per se* in the progression of AAA may be as yet unclear. Lastly, in animal models of AAAs induced by angiotensin II infusions, AAA formation has been shown to occur independently of the effects on blood pressure [17]. This suggests that other mechanisms, such as inflammatory and matrix degrading pathways, may be more important for the pathogenesis of AAA than changes in blood pressure in these settings. Thus, since ω-3 fatty acids do not appear to have a clinically significant effect on blood pressure and that the contribution of changes in blood pressure to AAA formation seems to be small, I decided to focus on tissue remodeling pathways in this study.

Another limitation of this study relates to the dose of EPA used and its effects on serum lipids. While the dose of EPA (10% wt/wt) used in this study is relatively high compared to that administered in humans, it is not markedly different from the doses and protocols used in other previous studies where the dose of EPA or fish oil administered to mice ranges from 2% to 27%, with 5% wt/wt diets the most commonly implemented protocol [44,49,65,82-84]. The serum concentration of EPA increases dramatically according to this feeding protocol, as reported extensively by Itoh *et al* and Matsumoto *et al* [49,83]. Using gas chromatography to measure the serum concentration of EPA, Itoh *et al* showed that the serum concentration of EPA after a 4-week 5% EPA diet increased from 5.30 to 260.78 μg/mL in wild-type mice and from 16.23 to 422.43 μg/mL in obese ob/ob mice [49]; these results were similar to those obtained by Matsumoto *et al* after feeding 5% EPA for 13-weeks to $ApoE^{-/-}$ mice [83], and together they demonstrate that oral feeding of EPA leads to a significant and reproducible increase in the serum concentration of EPA. The contribution of EPA's effect on serum lipids to suppression of AAA formation has also not been investigated in this study. Numerous studies in both humans and mice have reported that supplementation of EPA significantly reduces serum triglyceride levels with only minor reductions or no changes found in the total serum cholesterol levels [46,85,86]. Since

serum triglycerides and total serum cholesterol, both of which are risk factors for atherosclerosis, have been reported to be risk factors associated with AAAs [87], it is possible that the reduction in serum triglyceride after EPA supplementation may have affected the formation of AAAs in this study. However, given that the major findings in this study were seen at 1-week after AAA surgery (or 11 days after the start of experimental diets), effects of EPA on serum lipids may be outweighed by its effects on inflammatory and tissue remodeling pathways in the short term. Furthermore, since wild-type mice, which were used in this study, typically do not have significant atherosclerosis when on normal diets (that is, not an experimental high-fat diet), the usual effects of atherosclerosis and serum lipids on AAA formation may become even smaller particularly in the setting of an acute, inflammatory, and non-hyperlipidemic AAA model such as that used in this study. Nevertheless, reductions in serum lipids due to EPA may serve as an important contributing factor to suppression of AAA formation in the long-term, and dedicated long-term studies using hyperlipidemic AAA models (such as angiotensin II infusion in $ApoE^{-/-}$ mice) may be helpful in uncovering these effects in the future.

In conclusion, by using the $CaCl_2$-induced AAA model, I have shown that EPA can attenuate the formation of AAAs by directly suppressing AAA macrophage *Mmp9*

expression but not affecting absolute macrophage numbers. In addition, EPA also had a very clear effect in its inhibition of vascular calcification, an effect that is most likely mediated by the decrease in *Rankl* expression in AAAs of EPA-treated mice. Given the clinical prevalence of AAAs and the importance of vascular calcification in a variety of diseases, it is clear that future studies are needed to evaluate the use of EPA in AAA and vascular calcification prevention in humans. The fact that EPA is already in clinical use widely, both as a nutritional supplement in the form of unpurified fish oil preparations and as a pharmacological agent in the form of ultra-purified EPA, should facilitate further clinical studies.

7. ACKNOWLEDGMENTS

I gratefully thank Professor Issei Komuro and Professor Ryozo Nagai for their helpful and inspirational guidance and advice on the conduct, design as well as the interpretation of experimental results. This study would not have been possible without their input, time, and experience.

I would also like to thank Dr. Ichiro Manabe, Dr. Kosei Eguchi, Dr. Sahohime Matsumoto, and Dr. Katsuhito Fujiu in the Department of Cardiovascular Medicine for their helpful technical advice regarding the methodology, design, and interpretation of the results of this study.

8. REFERENCES

1. Siegel CL, Cohan RH, Korobkin M, Alpern MB, Courneya DL, et al. Abdominal aortic aneurysm morphology: CT features in patients with ruptured and nonruptured aneurysms. *Am J Roentgenol* 163:1123-1129 (1994).

2. U.S. Preventive Services Task Force. Screening for abdominal aortic aneurysm: recommendation statement. *Ann Intern Med* 142:198-202 (2005).

3. Sakalihasan N, Limet R and Defawe OD. Abdominal aortic aneurysm. *Lancet* 365:1577-1589 (2005).

4. Moll FL, Powell JT, Fraedrich G, Verzini F, Haulon S, et al. Management of Abdominal Aortic Aneurysms Clinical Practice Guidelines of the European Society for Vascular Surgery. *Eur J Vasc Endovasc Surg* 41, Supplement 1:S1-S58 (2011).

5. Multicentre Aneurysm Screening Study Group. Multicentre aneurysm screening study (MASS): cost effectiveness analysis of screening for abdominal aortic aneurysms based on four year results from randomised controlled trial. *BMJ* 325:1135 (2002).

6. Schermerhorn ML, O'Malley AJ, Jhaveri A, Cotterill P, Pomposelli F, et al.

Endovascular vs. Open Repair of Abdominal Aortic Aneurysms in the Medicare Population. *N Engl J Med* 358:464-474 (2008).

7. Miyake T and Morishita R. Pharmacological treatment of abdominal aortic aneurysm. *Cardiovasc Res* 83:436-443 (2009).

8. Lindeman JHN, Abdul-Hussien H, van Bockel JH, Wolterbeek R and Kleemann R. Clinical Trial of Doxycycline for Matrix Metalloproteinase-9 Inhibition in Patients With an Abdominal Aneurysm: Doxycycline Selectively Depletes Aortic Wall Neutrophils and Cytotoxic T Cells. *Circulation* 119:2209-2216 (2009).

9. Mosorin M, Juvonen J, Biancari F, Satta J, Surcel H-M, et al. Use of doxycycline to decrease the growth rate of abdominal aortic aneurysms: A randomized, double-blind, placebo-controlled pilot study. *J Vasc Surg* 34:606-610 (2001).

10. Vammen S, Lindholt JS, Østergaard L, Fasting H and Henneberg EW. Randomized double-blind controlled trial of roxithromycin for prevention of abdominal aortic aneurysm expansion. *Br J Surg* 88:1066-1072 (2001).

11. Rughani G, Robertson L and Clarke M. Medical treatment for small abdominal aortic aneurysms. *Cochrane Database Syst Rev* 9 (2012).

12. van der Meij E, Koning GG, Vriens PW, Peeters MF, Meijer CA, et al. A Clinical Evaluation of Statin Pleiotropy: Statins Selectively and Dose-Dependently Reduce Vascular Inflammation. *PLoS ONE* 8:e53882 (2013).

13. Gertz SD, Kurgan A and Eisenberg D. Aneurysm of the rabbit common carotid artery induced by periarterial application of calcium chloride in vivo. *J Clin Invest* 81:649-656 (1988).

14. Chiou AC, Chiu B and Pearce WH. Murine aortic aneurysm produced by periarterial application of calcium chloride. *J Surg Res* 99:371-376 (2001).

15. Daugherty A, Manning MW and Cassis LA. Angiotensin II promotes atherosclerotic lesions and aneurysms in apolipoprotein E-deficient mice. *J Clin Invest* 105:1605-1612 (2000).

16. Pyo R, Lee JK, Shipley JM, Curci JA, Mao D, et al. Targeted gene disruption of matrix metalloproteinase-9 (gelatinase B) suppresses development of experimental abdominal aortic aneurysms. *J Clin Invest* 105:1641-1649 (2000).

17. Daugherty A and Cassis LA. Mouse Models of Abdominal Aortic Aneurysms. *Arterioscler Thromb Vasc Biol* 24:429-434 (2004).

18. Kessenbrock K, Plaks V and Werb Z. Matrix Metalloproteinases: Regulators of the Tumor Microenvironment. *Cell* 141:52-67 (2010).

19. Yoshimura K, Aoki H, Ikeda Y, Fujii K, Akiyama N, et al. Regression of abdominal aortic aneurysm by inhibition of c-Jun N-terminal kinase. *Nat Med* 11:1330-1338 (2005).

20. Irizarry E, Newman KM, Gandhi RH, Nackman GB, Halpern V, et al. Demonstration of Interstitial Collagenase in Abdominal Aortic Aneurysm Disease. *J Surg Res* 54:571-574 (1993).

21. Newman KM, Ogata Y, Malon AM, Irizarry E, Gandhi RH, et al. Identification of matrix metalloproteinases 3 (stromelysin-1) and 9 (gelatinase B) in abdominal aortic aneurysm. *Arterioscler Thromb Vasc Biol* 14:1315-1320 (1994).

22. Newman KM, Jean-Claude J, Li H, Scholes JV, Ogata Y, et al. Cellular localization of matrix metalloproteinases in the abdominal aortic aneurysm wall. *J Vasc Surg* 20:814-820 (1994).

23. Curci JA, Liao S, Huffman MD, Shapiro SD and Thompson RW. Expression and localization of macrophage elastase (matrix metalloproteinase-12) in abdominal aortic aneurysms. *J Clin Invest* 102:1900-1910 (1998).

24. Koch AE, Haines GK, Rizzo RJ, Radosevich JA, Pope RM, et al. Human abdominal aortic aneurysms. Immunophenotypic analysis suggesting an immune-mediated response. *Am J Pathol* 137:1199-1213 (1990).

25. Longo GM, Xiong W, Greiner TC, Zhao Y, Fiotti N, et al. Matrix metalloproteinases 2 and 9 work in concert to produce aortic aneurysms. *J Clin Invest* 110:625-632 (2002).

26. Weintraub NL. Understanding abdominal aortic aneurysm. *N Engl J Med* 361:1114-1116 (2009).

27. Lin EY, Li J-F, Gnatovskiy L, Deng Y, Zhu L, et al. Macrophages Regulate the Angiogenic Switch in a Mouse Model of Breast Cancer. *Cancer Res* 66:11238-11246 (2006).

28. Weisberg SP, McCann D, Desai M, Rosenbaum M, Leibel RL, et al. Obesity is associated with macrophage accumulation in adipose tissue. *J Clin Invest* 112:1796-1808 (2003).

29. Gordon S and Taylor PR. Monocyte and macrophage heterogeneity. *Nat Rev Immunol* 5:953-964 (2005).

30. Geissmann F, Gordon S, Hume DA, Mowat AM and Randolph GJ. Unravelling mononuclear phagocyte heterogeneity. *Nat Rev Immunol* 10:453-460 (2010).

31. Mosser DM and Edwards JP. Exploring the full spectrum of macrophage activation. *Nat Rev Immunol* 8:958-969 (2008).

32. Fujiu K, Manabe I and Nagai R. Renal collecting duct epithelial cells regulate

inflammation in tubulointerstitial damage in mice. *J Clin Invest* 121:3425-3441 (2011).

33. Xiong W, Zhao Y, Prall A, Greiner TC and Baxter BT. Key Roles of CD4+ T Cells and IFN-γ in the Development of Abdominal Aortic Aneurysms in a Murine Model. *J Immunol* 172:2607-2612 (2004).

34. Shimizu K, Mitchell RN and Libby P. Inflammation and cellular immune responses in abdominal aortic aneurysms. *Arterioscler Thromb Vasc Biol* 26:987-994 (2006).

35. Eliason JL, Hannawa KK, Ailawadi G, Sinha I, Ford JW, et al. Neutrophil Depletion Inhibits Experimental Abdominal Aortic Aneurysm Formation. *Circulation* 112:232-240 (2005).

36. Sun J, Sukhova GK, Yang M, Wolters PJ, MacFarlane LA, et al. Mast cells modulate the pathogenesis of elastase-induced abdominal aortic aneurysms in mice. *J Clin Invest* 117:3359-3368 (2007).

37. Shimizu K, Shichiri M, Libby P, Lee RT and Mitchell RN. Th2-predominant inflammation and blockade of IFN-γ signaling induce aneurysms in allografted aortas. *J Clin Invest* 114:300-308 (2004).

38. Panizo S, Cardus A, Encinas M, Parisi E, Valcheva P, et al. RANKL increases

vascular smooth muscle cell calcification through a RANK-BMP4–dependent pathway. *Circ Res* 104:1041-1048 (2009).

39. Collin-Osdoby P. Regulation of vascular calcification by osteoclast regulatory factors RANKL and osteoprotegerin. *Circ Res* 95:1046-1057 (2004).

40. Byon CH, Sun Y, Chen J, Yuan K, Mao X, et al. Runx2-upregulated receptor activator of nuclear factor kappaB ligand in calcifying smooth muscle cells promotes migration and osteoclastic differentiation of macrophages. *Arterioscler Thromb Vasc Biol* 31:1387-1396 (2011).

41. Sun Y, Byon CH, Yuan K, Chen J, Mao X, et al. Smooth Muscle Cell–Specific Runx2 Deficiency Inhibits Vascular Calcification. *Circ Res* 111:543-552 (2012).

42. Kris-Etherton PM, Harris WS, Appel LJ and for the Nutrition Committee. Fish consumption, fish oil, omega-3 fatty acids, and cardiovascular disease. *Circulation* 106:2747-2757 (2002).

43. Schwab JM, Chiang N, Arita M and Serhan CN. Resolvin E1 and protectin D1 activate inflammation-resolution programmes. *Nature* 447:869-874 (2007).

44. Oh DY, Talukdar S, Bae EJ, Imamura T, Morinaga H, et al. GPR120 is an omega-3 fatty acid receptor mediating potent anti-inflammatory and insulin-sensitizing effects. *Cell* 142:687-698 (2010).

45. Chen J, Shearer GC, Chen Q, Healy CL, Beyer AJ, et al. Omega-3 fatty acids prevent pressure overload-induced cardiac fibrosis through activation of cyclic GMP/protein kinase G signaling in cardiac fibroblasts. *Circulation* 123:584-593 (2011).

46. Yokoyama M, Origasa H, Matsuzaki M, Matsuzawa Y, Saito Y, et al. Effects of eicosapentaenoic acid on major coronary events in hypercholesterolaemic patients (JELIS): a randomised open-label, blinded endpoint analysis. *Lancet* 369:1090-1098 (2007).

47. Saravanan P, Davidson NC, Schmidt EB and Calder PC. Cardiovascular effects of marine omega-3 fatty acids. *Lancet* 376:540-550 (2010).

48. Serhan CN, Chiang N and Van Dyke TE. Resolving inflammation: dual anti-inflammatory and pro-resolution lipid mediators. *Nat Rev Immunol* 8:349-361 (2008).

49. Itoh M, Suganami T, Satoh N, Tanimoto-Koyama K, Yuan X, et al. Increased adiponectin secretion by highly purified eicosapentaenoic acid in rodent models of obesity and human obese subjects. *Arterioscler Thromb Vasc Biol* 27:1918-1925 (2007).

50. Hu X and Beeton C. Detection of functional matrix metalloproteinases by

zymography. *J Vis Exp*:e2445 (2010).

51. Ray A and Dittel BN. Isolation of Mouse Peritoneal Cavity Cells. *J Vis Exp*:e1488 (2010).

52. Eguchi K, Manabe I, Oishi-Tanaka Y, Ohsugi M, Kono N, et al. Saturated fatty acid and TLR signaling link β cell dysfunction and islet inflammation. *Cell Metab* 15:518-533 (2012).

53. Magnusson MK and Mosher DF. Fibronectin: Structure, assembly, and cardiovascular implications. *Arterioscler Thromb Vasc Biol* 18:1363-1370 (1998).

54. Thompson RW, Holmes DR, Mertens RA, Liao S, Botney MD, et al. Production and localization of 92-kilodalton gelatinase in abdominal aortic aneurysms. An elastolytic metalloproteinase expressed by aneurysm-infiltrating macrophages. *J Clin Invest* 96:318-326 (1995).

55. Lin SL, Castano AP, Nowlin BT, Lupher ML, Jr. and Duffield JS. Bone Marrow Ly6Chigh Monocytes Are Selectively Recruited to Injured Kidney and Differentiate into Functionally Distinct Populations. *J Immunol* 183:6733-6743 (2009).

56. Sato K, Suematsu A, Nakashima T, Takemoto-Kimura S, Aoki K, et al.

Regulation of osteoclast differentiation and function by the CaMK-CREB pathway. *Nat Med* 12:1410-1416 (2006).

57. GISSI-Prevenzione Investigators. Dietary supplementation with n-3 polyunsaturated fatty acids and vitamin E after myocardial infarction: results of the GISSI-Prevenzione trial. *Lancet* 354:447-455 (1999).

58. GISSI-HF Investigators. Effect of n-3 polyunsaturated fatty acids in patients with chronic heart failure (the GISSI-HF trial): a randomised, double-blind, placebo-controlled trial. *Lancet* 372:1223-1230 (2008).

59. Bønaa KH, Bjerve KS, Straume B, Gram IT and Thelle D. Effect of eicosapentaenoic and docosahexaenoic acids on blood pressure in hypertension. *N Engl J Med* 322:795-801 (1990).

60. Pradelli L, Mayer K, Muscaritoli M and Heller A. n-3 fatty acid-enriched parenteral nutrition regimens in elective surgical and ICU patients: a meta-analysis. *Crit Care* 16:R184 (2012).

61. Donadio JV, Bergstralh EJ, Offord KP, Spencer DC and Holley KE. A controlled trial of fish oil in IgA nephropathy. *N Engl J Med* 331:1194-1199 (1994).

62. Allaire E, Forough R, Clowes M, Starcher B and Clowes AW. Local overexpression of TIMP-1 prevents aortic aneurysm degeneration and rupture in

a rat model. *J Clin Invest* 102:1413-1420 (1998).

63. Defawe OD, Colige A, Lambert CA, Munaut C, Delvenne P, et al. TIMP-2 and PAI-1 mRNA levels are lower in aneurysmal as compared to athero-occlusive abdominal aortas. *Cardiovasc Res* 60:205-213 (2003).

64. Arnardottir HH, Freysdottir J and Hardardottir I. Dietary Fish Oil Decreases the Proportion of Classical Monocytes in Blood in Healthy Mice but Increases Their Proportion upon Induction of Inflammation. *J Nutr* 142:803-808 (2012).

65. Blok WL, de Bruijn MF, Leenen PJ, Eling WM, van Rooijen N, et al. Dietary n-3 fatty acids increase spleen size and postendotoxin circulating TNF in mice; role of macrophages, macrophage precursors, and colony-stimulating factor-1. *J Immunol* 157:5569-5573 (1996).

66. Wang S, Zhang C, Zhang M, Liang B, Zhu H, et al. Activation of AMP-activated protein kinase alpha2 by nicotine instigates formation of abdominal aortic aneurysms in mice in vivo. *Nat Med* 18:902-910 (2012).

67. Byon CH, Sun Y, Chen J, Yuan K, Mao X, et al. Runx2-upregulated Receptor Activator of Nuclear Factor κB Ligand in calcifying smooth muscle cells promotes migration and osteoclastic differentiation of macrophages. *Arterioscler Thromb Vasc Biol* 31:1387-1396 (2011).

68. Kim HH, Lee Y, Eun HC and Chung JH. Eicosapentaenoic acid inhibits TNF-[alpha]-induced matrix metalloproteinase-9 expression in human keratinocytes, HaCaT cells. *Biochem Biophys Res Commun* 368:343-349 (2008).

69. Mishra A, Chaudhary A and Sethi S. Oxidized Omega-3 Fatty Acids Inhibit NF-κB Activation Via a PPARα-Dependent Pathway. *Arterioscler Thromb Vasc Biol* 24:1621-1627 (2004).

70. Zhao Y, Joshi-Barve S, Barve S and Chen LH. Eicosapentaenoic Acid Prevents LPS-Induced TNF-α Expression by Preventing NF-κB Activation. *J Am Coll Nutr* 23:71-78 (2004).

71. Chapkin RS, Kim W, Lupton JR and McMurray DN. Dietary docosahexaenoic and eicosapentaenoic acid: Emerging mediators of inflammation. *Prostaglandins Leukot Essent Fatty Acids* 81:187-191 (2009).

72. Smith WL. Cyclooxygenases, peroxide tone and the allure of fish oil. *Curr Opin Cell Biol* 17:174-182 (2005).

73. Wang M, Lee E, Song W, Ricciotti E, Rader DJ, et al. Microsomal Prostaglandin E Synthase-1 Deletion Suppresses Oxidative Stress and Angiotensin II–Induced Abdominal Aortic Aneurysm Formation. *Circulation* 117:1302-1309 (2008).

74. Walton LJ, Franklin IJ, Bayston T, Brown LC, Greenhalgh RM, et al. Inhibition

of Prostaglandin E2 Synthesis in Abdominal Aortic Aneurysms : Implications for Smooth Muscle Cell Viability, Inflammatory Processes, and the Expansion of Abdominal Aortic Aneurysms. *Circulation* 100:48-54 (1999).

75. King VL, Trivedi DB, Gitlin JM and Loftin CD. Selective Cyclooxygenase-2 Inhibition With Celecoxib Decreases Angiotensin II-Induced Abdominal Aortic Aneurysm Formation in Mice. *Arterioscler Thromb Vasc Biol* 26:1137-1143 (2006).

76. Renò F and Cannas M. Effect of prostaglandin E2 on PMA-induced macrophage differentiation. *Prostaglandins Other Lipid Mediat* 75:13-24 (2005).

77. Li W, Unlugedik E, Bocking AD and Challis JRG. The Role of Prostaglandins in the Mechanism of Lipopolysaccharide-Induced proMMP9 Secretion from Human Placenta and Fetal Membrane Cells. *Biol Reprod* 76:654-659 (2007).

78. Yen J-H, Kocieda VP, Jing H and Ganea D. Prostaglandin E2 Induces Matrix Metalloproteinase 9 Expression in Dendritic Cells through Two Independent Signaling Pathways Leading to Activator Protein 1 (AP-1) Activation. *J Biol Chem* 286:38913-38923 (2011).

79. Morris MC, Sacks F and Rosner B. Does fish oil lower blood pressure? A meta-analysis of controlled trials. *Circulation* 88:523-533 (1993).

80. Iribarren C, Darbinian JA, Go AS, Fireman BH, Lee CD, et al. Traditional and Novel Risk Factors for Clinically Diagnosed Abdominal Aortic Aneurysm: The Kaiser Multiphasic Health Checkup Cohort Study. *Ann Epidemiol* 17:669-678 (2007).

81. Baxter BT, Terrin MC and Dalman RL. Medical Management of Small Abdominal Aortic Aneurysms. *Circulation* 117:1883-1889 (2008).

82. Connor KM, SanGiovanni JP, Lofqvist C, Aderman CM, Chen J, et al. Increased dietary intake of [omega]-3-polyunsaturated fatty acids reduces pathological retinal angiogenesis. *Nat Med* 13:868-873 (2007).

83. Matsumoto M, Sata M, Fukuda D, Tanaka K, Soma M, et al. Orally administered eicosapentaenoic acid reduces and stabilizes atherosclerotic lesions in ApoE-deficient mice. *Atherosclerosis* 197:524-533 (2008).

84. Nakajima K, Yamashita T, Kita T, Takeda M, Sasaki N, et al. Orally Administered Eicosapentaenoic Acid Induces Rapid Regression of Atherosclerosis Via Modulating the Phenotype of Dendritic Cells in LDL Receptor-Deficient Mice. *Arterioscler Thromb Vasc Biol* 31:1963-1972 (2011).

85. Saynor R and Verel D. Eicosapentaenoic acid, bleeding time, and serum lipids. *Lancet* 320:272 (1982).

86. Saynor R, Verel D and Gillott T. The long-term effect of dietary supplementation with fish lipid concentrate on serum lipids, bleeding time, platelets and angina. *Atherosclerosis* 50:3-10 (1984).

87. Wanhainen A, Bergqvist D, Boman K, Nilsson TK, Rutegård J, et al. Risk factors associated with abdominal aortic aneurysm: A population-based study with historical and current data. *J Vasc Surg* 41:390-396 (2005).